EFFICIENT WIRELESS POWER TRANSFER FOR LOW POWER WIDE AREA NETWORKS

Molefi Johannes Makhetha

Dissertation submitted in fulfilment of the requirements for the degree:

MASTER OF ENGINEERING: ENGINEERING: ELECTRICAL

in the

Department of Electrical, Electronic and Computer Engineering

Faculty of Engineering, Built Environment and Information Technology

at the

Central University of Technology, Free State

Supervisor: Prof. Elisha D. Markus

Co-supervisor: Prof. Adnan M. Abu-Mahfouz

Bloemfontein
2021

Declaration

I, MOLEFI JOHANNES MAKHETHA, student number _____, do hereby declare that this research project, which has been submitted to the Central University of Tech-nology Free State, for the degree: Master of Engineering in Electrical Engineering, is my own independent work and complies with the Code of Academic Integrity, as well as other relevant policies, procedures, rules and regulations of the Central University of Technology, Free State. This project has not been submitted before by any person in fulfilment (or partial fulfilment) of the requirements for the attainment of any qualification.

Molefi Johannes Makhetha
Date: April 2021

Acknowledgements

My sincere gratitude to my major supervisor, Prof. Elisha D. Markus, for his supervision and encouragement throughout my Masters program. He provided me with positive academic advice and the latest research tools, which allowed me to improve the quality of my research. I am also appreciative of Prof. Adnan M. Abu-Mahfouz for being part of this research and for his formidable inputs.

I am most of all grateful for my family especially my mom, who encouraged me during the research. Without their undivided support, it would have been difficult for me to conduct this research journey. I would specifically like to point out the guidance of Nkopane Isaac Makhetha and Matshediso Mokoena for their incomparable leadership and help throughout the years of my Study. I am also deeply thankful to the Council for Scientific and Industrial Research (CSIR) for granting me the financial support and educational guidance. Finally, I would like to thank the Central University of Technology Graduate School for their support through workshops and webinars, components, grants and their constructive feedback throughout my study.

Dedication

I devote this dissertation to my beloved family. Without their guidance, kindness and encouragement, this work would have never became a reality ....

Abstract

Wireless power transfer (WPT) technologies for small devices and low power sensors have drawn substantial research attention in recent years. Traditional near and far-field WPT systems cannot provide efficient-high power transfer while at the same time maintaining long range power transfer. A possible candidate to overcome these challenges is the strongly coupled magnetic resonance (SCMR) WPT technique which can transfer power at higher transmission efficiency in the medium range. Heretofore, the focus has been to improve the efficiency and range of the SCMR system. On the other hand, the study to develop optimal coils or loops of the WPT system utilising less computational resources as well as using co-simulations between less and high intense software has been limited. More so, the existing WPT systems are complex and bulky in size making it a challenge to use these technologies for small footprint applications. Therefore, innovative SCMR systems that are designed to be easy to fabricate and with low losses and of small footprint will notably improve various technologies in a variety of applications.

The optimal and small footprint SCMR WPT systems are studied in this work. The analytical models of the Conformal-SCMR (CSCMR) system are presented first through design methodology and analysis. The designed CSCMR systems' performance is envisaged from the identified optimal design parameters through this analysis. Furthermore, the derived optimal parameters are fabricated, analysed and compared in a 3D simulator, a conventional CSCMR model and a 2-layer self-resonant resonator model. It was noted that the 2-layer self-resonant model performed better than the conventional model and this was verified by mathematical formulae and equivalent circuit models. The two models were then optimised using their derived physical parameters. This was done through a co-simulation. The results showed that the co-simulation increased the simulation speeds, therefore saving computational resources. In conclusion, the two optimised model's transmission efficiency was improved by 30% and 4% for the conventional derived and the 2-layer self-resonant CSCMR-WPT systems. This was achieved while the footprint of these systems was reduced.

Contents

List of Figures

List of Tables

Chapter 1

Introduction

1.1 Background and Motivation

Wireless systems have been researched more in the past decade due to their non-destructiveness and simplicity. Particularly, advances in semiconductor technology and wireless communication have allowed a wide variety of industrial devices, medical, and portable consumer electronics. Apart from the traditional ways of powering electronic devices such as utilising wires as primary power transmission medium, wireless power transfer (WPT) is a promising power transfer technique. There are presently four mainstream WPT technologies: wireless energy transfer combined inductively, WPT via strongly coupled magnetic resonant (SCMR), microwave radiation and laser. Among the four techniques, SCMR has proven to be more effective for applications of short to medium distances and has less electromagnetic radiation than other techniques [7]. Some possible applications of strongly coupled magnetic resonance WPT (SCMR-WPT) include low power wide area networks (LPWAN) such as long-range wide area network (LoRaWAN) end-devices which can be used in structural health monitoring (SHM), and medical wearable devices (MWD). LPWAN systems are inexpensive to deploy and can be applied through long distances and consume very low power. These systems have revolutionised the internet of things (IoT) because of the aforementioned attributes.

Applications of LPWAN systems such as water quality monitoring (WQM), SHM [1, 2] and human health monitoring (HHM) have helped reduce the intensity of unforeseen events such as contaminated drinking water, failing of large structures (flats, bridges and malls) without prior warnings which may cost considerable amounts of money and great loss of life. For the above mentioned LPWAN systems applications, real-time monitoring can locate potential faults and provide warnings on time and send alerts to the relevant sources, which in turn will respond and correct the potential threat on time, saving lives in the process. These sensors can evaluate and give feedback on certain parameters such as, water pH levels and turbidity (for WQM), temperature, stress, force, displacement (for SHM) [3], patient management and disease management (for HHM) [4]. Traditional sensors, on the other hand, are connected to the central station through wires, which power the sensors and recoup their data. Installation of traditional wired sensors takes too much time and is costly. The installation of wires takes nearly 75% of the connection time and totals up to 25% of the total cost [5]. Furthermore, if some of the connection wires are destructed, whether by loose connections or by some wires being corroded, the whole system becomes inoperable. Hence, efficient techniques and methods for wireless sensors need to be developed to provide reliable and cost-effective monitoring systems.

LPWAN devices have a great potential for providing low cost and long distance wireless sensing abilities. Conversely, one main challenge of LPWAN devices involves power supply of the sensors, whether embedded or on surface. Traditionally, the use of batteries as the primary source of power for LPWAN devices has been most common, however batteries wear off with time. Moreover, it becomes difficult to replace batteries when the sensors are embedded in a solid structure or when sensors are installed in dangerous places. Thus, efficient wireless powering solutions that can charge sensor batteries and which can extend the operating lifespan of the sensors are needed. Most WPT systems

are complex to develop and have bulky physical dimensions which makes it difficult to apply for small devices. Hence, small-scale WPT systems which can be utilised at low frequencies while exhibiting high efficiencies need to be analysed. Also, LPWAN devices face challenges when there are other high frequency devices operating in their vicinity, which makes it even more important to find WPT solutions operating at low frequencies.

1.2 Problem Statement

Power transfer distance and misalignments between the transmitter and receiver contribute to performance and convenience in a (WPT) system. In most cases, the transfer or transmission distance and efficiency of a WPT are inversely square related. More so, when data communication is conducted concurrently with WPT, large interference signals may be induced which degrade performance significantly. The interference that is caused by LPWANs when in proximity with WPT devices, could be overcome by increasing the distance between the transmitter and receiver coils of the WPT system. However, this reduces the efficiency of the WPT. The challenge of transferring power efficiently when the distance between the transmitter and the receiver increases is still an open problem.

1.3 Research Objectives

The goal of this research is to develop an efficient WPT system for powering LPWAN devices and to overcome the disadvantages of the existing WPT systems such as bulkiness and high operating frequencies which can cause disturbance to LPWAN devices. It is based on SCMR and the main aspects of this work are:

1. To investigate the four-coil SCMR-WPT systems and their performances.

2. Develop analytic SCMR systems model. The impact of dimension parameters on transmission efficiency and frequency will be discussed. As a function of geometrical

and material parameters, the efficiency of SCMR systems is calculated using the proposed analytical model. As a result of this analysis, geometrical parameters of SCMR WPT systems that provide maximum efficiency are identified.

3. To analyse electrical parameters such as self-inductance (L), mutual induction (M) and quality factor (Q) influence on the power transfer efficiency.

1.4 Contributions

This dissertation contributes to scholarly knowledge in the following ways:

1. A less computational resource-intensive resonator model is derived and simulated using MATLAB, this method is quicker and more accurate than conceptualising a loop resonator from a 3D capable software which requires intensive computational time and resources.

2. A Conformal SCMR (CSCMR) WPT system operating at low frequency industrial, scientific and medical (ISM) band of 40.68 MHz is proposed, utilising lumped capacitors to operate efficiently at low frequencies. Lower operating frequencies emit less radiation which is safe for the environment.

3. A two-layer CSCMR-WPT self-resonant model is also analysed and compared with a capacitor loaded model.

4. No tuning equipment is required to operate the WPT system at the selected resonant frequency, which makes the whole system less bulky and minimises cost.

1.5 Research Methodology

1.5.1 Theoretical Analysis

An analysis to comprehend the theory of WPT and its mathematical underpinnings were conducted. During this analysis, the physical dimensions such as loop width, loop thickness, outermost diameter of the loop as well as electrical parameters such as the self-inductance, mutual inductance and quality factor dependencies were explored. The effects of mutual inductance and coupling coefficient (a function of self-inductance of each adjacent loops and the mutual inductance between them) on transmission efficiency of the WPT were systematically analysed at different separation distances. The physical dimensions of the resonators (transmitter (Tx) and receiver (Rx)) were identical and the source and load loops followed the same trend.

1.5.2 Optimal Loop Derivation

With the mathematical analysis performed, the derived mathematical formulae were then analysed using MATLAB code to determine the optimal resonator loop parameters. The analysis conducted in MATLAB were then compared with the traditional method of analysing WPT systems in terms of the computational time taken to run the analysis with accuracy and the computational resources used when compared to a 3D simulating software. To get a broader view on finding the optimal loop which translates to an optimal WPT, a capacitor-loaded and a self-resonant wireless power transfer systems were compared by taking into account their power transmission efficiency, footprint (bulkiness) and material needed such as capacitors.

1.5.3 Simulations

The derived optimal resonator loop was built in a 3D electromagnetic simulator High-Frequency Structure Simulator (HFSS). Then, the resonator was fine-tuned to adhere to

the physical constraints of this study to realise a small footprint WPT. The resonator loop was then designed in such a way that the source or the load loops fit concentrically inside.

Co-simulation Between HFSS and OptiSLang

In order to find the optimal source/load loop, the loop was constructed to fit concentrically inside the resonator loop. This combined system took much computational resources. Therefore, to find the best fit source/load loop, the co-simulation was performed to decrease the simulation time and to ease the high use of computational resources. The optimisation was then run in OptiSLang using the surrogate model of the system to reduce the simulation time even further while the accuracy of the optimisation was observed in relation to the physical constraints. The optimised resonator with the source/load loop consideration was then fine-tuned in HFSS. Further, the complete WPT system consisting of four loops, which comprised two resonators (identical), a source loop and the load loop were simulated and fine-tuned in HFSS. The whole system performance was then analysed, focusing on the scattering parameters (transmission coefficient S21) which is the function of transmission efficiency.

1.6 List of Publications and Presentations

1. Makhetha M., Markus ED., Abu-Mahfouz, Adnan, "Wireless Power Transfer for IoT Devices-A Review", *2019 International Multidisciplinary Information Technology and Engineering Conference (IMITEC)*, Vaal University of Technology, South Africa, 2019.

2. Makhetha M., Markus ED., Abu-Mahfouz, Adnan, "Wireless power transfer for LoRa low-power wide-area networks (LPWANs)", *2019 Southern African Universities Power Engineering Conference/Robotics and Mechatronics/Pattern Recognition Association of South Africa (SAUPEC/RobMech/PRASA)*, Bloemfontein, South

Africa, 2019.

3. Makhetha M., Markus ED., Abu-Mahfouz, Adnan, "Accelerated Design of a Conformal Strongly Coupled Magnetic Resonance Wireless Power Transfer", *24TH INTERNATIONAL CONFERENCE ON INFORMATION FUSION*, 2021. [accepted for publication]

4. Makhetha M., Markus ED., Abu-Mahfouz, Adnan, "Efficient Wireless Power Transfer via Self-resonant Conformal Strongly Coupled Magnetic Resonance for Wireless Sensor Networks", *MDPI Sensors Journal*, 2021. [accepted for publication]

1.7 Dissertation Outline

This dissertation is organised as follows. A general background on WPT and charging LPWAN devices is provided in chapter 2. Short and long range WPT systems are reviewed as well as applications. In Chapter 3, mathematical formulae are derived and optimal equivalent WPT models are derived through formulation. Chapter 4 shows the systematic optimisation of the derived loop resonator, then the source and load loops are parametrically derived based on the systems constraints and the resonators' limits. Thereafter, a full WPT system is simulated and further tuned to yield optimal transmission efficiency. Chapter 5 summarises the conclusions of this research and identifies future research directions.

Chapter 2

Literature Review

In this chapter, an overview on wireless power transfer (WPT) is given. The history of the power transfer technique is presented first in section 2.1 followed by different WPT systems in section 2.2. These include long range radiative techniques in section 2.3 as well as medium to short range non-radiative techniques in section 2.4. Applications of WPT are then detailed in section 2.5 whereby industrial, automotive, aerospace, medicine, consumer electronics, wireless sensor networks and low power wide area networks form part of these applications. The standards that guide these systems are also discussed in section 2.6. Lastly, WPT for small electronics is presented in section 2.7 which elaborates further the application of wireless power using strongly coupled magnetic resonance.

2.1 Wireless Power Transfer History

This section provides a summary of the history of WPT. H.C Oersted, a Danish physicist and chemist, performed the first published WPT experiment in 1819 [6]. In his experiment, Oersted demonstrated that the magnetic field of proportional magnitude will be produced around the conductor when the current flows through the conductor. Faraday's Law of induction was later developed followed by Biot-Savart's Law and Ampere's Force

Law, emphasising the relationship between magnetism and electric current [7].

The classical foundation of electromagnetism was formed in 1864 when J.C. Maxwell described how the electric and magnetic field are produced and affected mathematically by each other and outlined them by Maxwell's equations. His magnetism and electricity theory together with his other research work throughout his career at Cambridge University were compiled into a publication "A Treatise on Electricity and Magnetism" [8] later in 1873. He concluded in his study that magnetism and electricity are controlled by the same force.

Throughout his ground-breaking work evaluating Maxwell's equations, a German scientist H.R. Hertz, effectively utilised a set of oscillators to transmit electrical power past a tiny opening between the coils in 1888 [9]. This experiment being the first ever to practically confirm Maxwell's predictions of electromagnetic radiation existence, was a breakthrough. Nikola Tesla, a Croatian-born American researcher who spent the majority of his time experimenting, carried out a series of experiments focused on electromagnetic radiation. Nikola Tesla's main objective was to develop a sustainable wireless power transfer over long distance. In 1891, his first patent was filled for a high frequency lighting system which only uses a one wire as conductor to light a single terminal carbon lamp without a return wire [10]. In 1899, Tesla made yet another breakthrough by transferring 108V of high-frequency electric power across the stage to switch on Geissler tubes [11]. The "Tesla Coil" with an air spacing between the coils, was one of Tesla's inventions during his research based on wireless transfer of electricity, which was developed for the purpose of transmitting electricity through the ionosphere over wider distances. However, the project was eventually shut down due to safety concerns, low performance, and funding concerns sparked by a breakthrough made by an Italian researcher, Marconi, who was able to successfully transmit a radio signal across the Atlantic Ocean [12].

In 1910, H Gerdien was involved in the initial invention of magnetron and more and more devices possessing the same principles followed in the following decades after that. Though the design was able to convert electricity to microwave which has the potential to transmit energy over long distances, conversion of microwave to electricity remained a challenge. In 1964, W.C Brown, a specialist in the magnetron theory, discovered a method for converting incident microwave power to dc power through a rectenna [13].

From the time when the rectenna was developed, more efforts have been made to transmit power wirelessly at longer distances. As the WPT research gained more momentum, in 1975, Brown effectively transmitted 30 kW over 1.61 km using microwave with an efficiency of 84% [14]. However, due to the development of solar power satellites which were first described in 1968, Brown's research had to be superseded [15]. The basic idea behind a solar power satellite is to position a large geostationary satellite in Earth's orbit that collects solar energy and then transfers it to Earth through microwaves. For low-power appliances, a coupling-based electromagnetic transmission technique was proposed, and this technique was incorporated in a medical implantable system [16].

There has been tremendous portable electronics development during the past two decades with their prices dropping as there have been advancements in semiconductor theory. With these advancements, portable devices are getting smaller which becomes more convenient for a vast utilisation by consumers. The only challenge is the powering methods such as the mostly utilised wire plug in power feed and the use of batteries. Since batteries have a finite amount of power and a finite lifetime, low-power inductive-based wireless power transfer has been proposed [17]. However, in 2007, Professor Marin Soljačić and his team of researchers demonstrated a non-radiative phenomenon of midrange WPT using magnetically coupled coils [18]. The speedy advancements of WPT techniques will not only offer consumers the convenience but it will also cater into the rapid further developments of miniaturisation of portable devices, medical implantable devices et cetera.

The demand for efficient short to mid-range WPT has been growing exponentially with the introduction of more WPT capable devices such as wireless sensor network devices, electric vehicles and portable devices just to name a few. This has led to a situation where WPT systems had to comply with international standards which ensures safety. Today there are three different standards which have been employed in the market with the most popular one being the Qi standard which was introduced by the Wireless Power Consortium (WPC) [19]. The standard uses the frequency bands within 115 to 300 kHz for WPT charging of up to 10 W (5V, 2A). Also, the Alliance for Wireless Power (A4WP) and Power Matters Alliance (PMA) have their standards as well and utilises 6.78 MHz and 87 to 357 kHz frequency bands for power transfer respectively [20].

2.2 Wireless Power Transfer Techniques

There are two WPT classifications: long range (radiative) and short range (non-radiative) techniques. Figure 2.1 shows these classifications of WPT techniques.

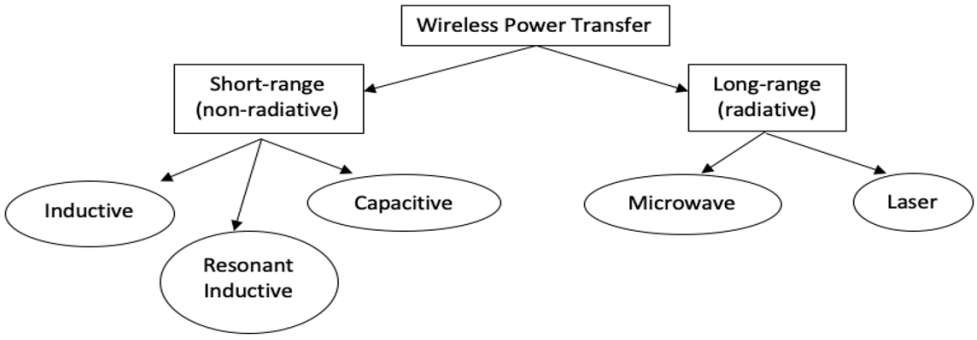

Figure 2.1: Wireless Power Transfer classifications.

Figure 2.1 depicts how the two strategies can be further subdivided into two distinct sub-categories. The long-range WPT uses an optical beam or a radio frequency wave to transmit power, while the short-range WPT uses magnetic induction or capacitive charge.

2.3 WPT through electromagnetic radiation

Radiative WPT is a long-range technique where power is transferred over long distances. This approach uses very high frequencies end of the spectrum via electromagnetic (EM) waves, such as X-ray, infra-red or microwave. A distinctive radiative WPT frequency band falls in the range of 300 MHz to 1000 GHz.

2.3.1 Microwaves

Microwave wireless power transfer (MWPT) has the ability to transfer energy over long distances from km to tens of km with considerably sound efficiency. Raytheon Company saw the initial deployment of microwave WPT in 1858. Hollow wave-guides and coaxial lines are examples of circuits connected to wave propagation, with substantially lesser wavelengths which can be scattered, thus, the transmission distances can be longer [21]. The way MWPT works is such that microwave generator converts direct current (DC) to microwaves, which are then transmitted via coax to the wave-guide adapter, allowing the wave generator to be isolated and the selected frequency not to be detuned [15]. Directional couplers and tuners are used to distinguish between waves that are targeted towards the receiver antenna based on propagation directions. Then a low pass filter is used to pass the signal upon its arrival and the received microwave energy is converted back to an electrical energy. Although the bandwidth of 2.45 GHz has been proved to have the highest efficiency above 90% to be used in MWPT [22], 5.8 GHz, 8.5 GHz, 10GHz and 35 GHz are also considered and with good efficiencies for MWPT. Additionally, the rectenna and microwave generator used to transmit power have a significant impact on MWPT performance.

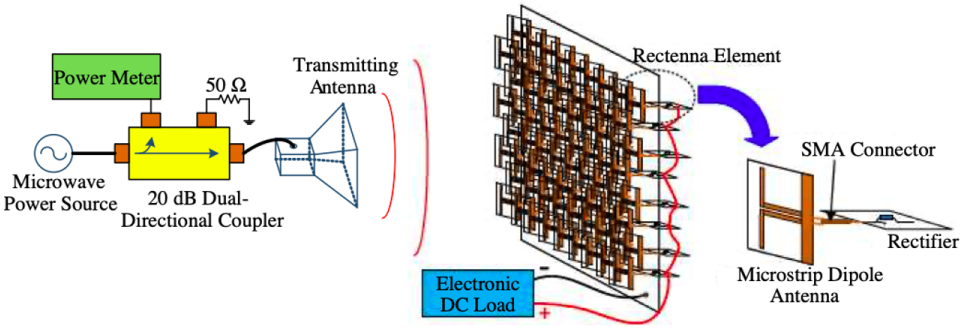

Figure 2.2: Microwave WPT [23].

MWPT has the ability to transfer power over long distances. Yet, for efficient power to be delivered from the transmitter to the receiver, there must be a clear alignment between the transmitter and receiver which simply means that at all times when transmission is taking place, the transmitter must be aligned to the receiver. [22]. Safety is the main concern on the use of MWPT as it poses danger to the human body and other organisms [24]. The major applications of MWPT include solar power satellites (SPS), space exploration missions and unmanned ground vehicles.

2.3.2 Laser

Laser WPT is mostly researched in military applications. Electrical current is converted to high density light and then transferred by pointing a light beam to a high performance photovoltaic cell, which acts as a receiver, in order for transmission to take place. As the light is received, it is then converted to electricity. In the visible or near infrared frequency range, laser energy takes advantage of the atmospheric transparency window [25]. Laser WPT usually has low efficiencies because the energy transmitted gets lost in the atmosphere and weather conditions play a role in the low efficiency.Until recently, few studies on laser beams for WPT had been carried out. The authors in [26] utilised laser for charging of an unmanned aerial vehicle (UAV) to maximise its operability. As detailed in Figure 2.3 a UAV-enabled device receiving power via laser WPT.

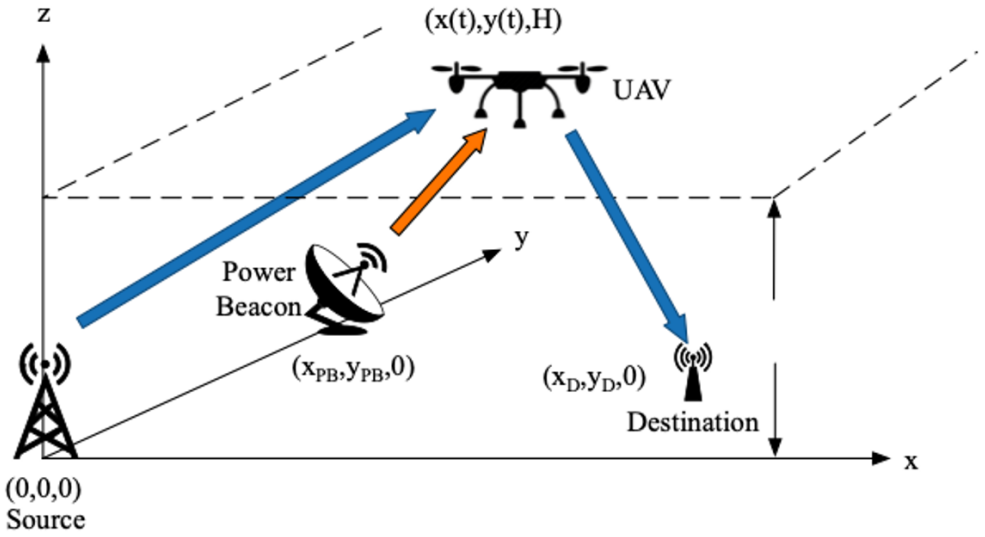

Figure 2.3: UAV system with a laser power beacon [26].

Laser WPT, like microwaves, necessitates precise transmitter-receiver alignment [27, 28]. The efficiency of laser WPT is usually low falling somewhere within 40-50%. Atmospheric absorption highly effects the light beams hence in some instances the power transmitted can be absorbed by the atmosphere before it is even received [29]. The above-mentioned phenomenon can be referred as transmission attenuation where power decreases because of the distance or air quality. Laser, again like MWPT, is harmful to the human body as the power density is brighter than the equivalent area of the sun's surface, therefore laser can cause injury to the eyes (retina) if it stays on one spot for few seconds [30]. Some of the applications of laser WPT include unmanned ground vehicles (UGVs), direct energy weapon and satellites.

2.4 Non-radiative WPT through Non-radiative

2.4.1 Inductive Coupling

Inductive coupling power transfer (ICPT) is a short-range wireless power transmission technique that uses inductive coupling. This technique typically operates within distances of millimetres to centimetres while its operating frequency band falls within 80-300 kHz.

The ICPT uses the magnetic field, caused by an alternating current (AC) to transfer energy between the coils made of wire which creates an output voltage in the receiving coil [31]. The power received by the receiving coil is usually used to charge a battery or used by the device. The coils usually have a low quality-factor because the transferred power attenuates quickly if the quality factor of the coils is high [32]. For the ICPT to function properly, the distance between the coils must be short, usually less than the transmitter coil diameter. The increase in distance will cause the system to be inefficient.

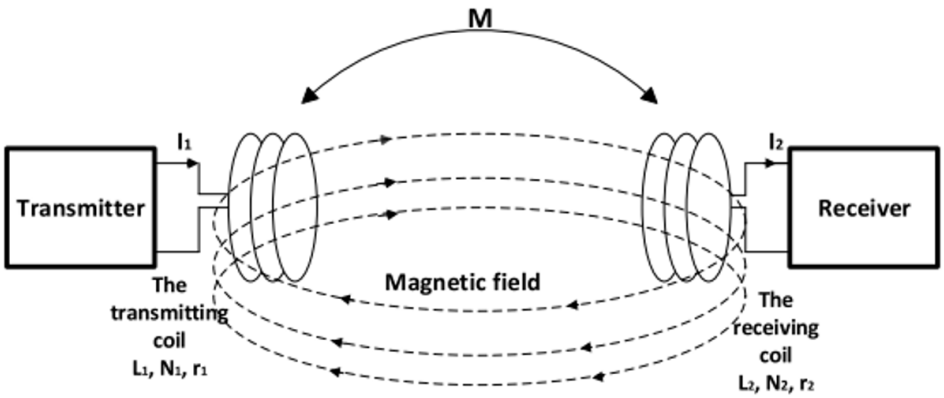

Figure 2.4: Typical inductive coupling WPT system [31].

The main advantage of using ICPT in the wireless power transfer paradigm is that it eliminates the use of wires. Additionally, since more research has gone into the ICPT, its systems are more optimised and therefore convenient for power supply and charging [33]. ICPT is also very easy to use, to charge a device, the charging pad can be plugged into the power unit, and the transmitter can then be attached to the battery [34]. Companies like Apple, Samsung, Huawei, and many more, already ship most of their products with the capability for WPT. In most instances, since it allows the system to be shielded from the outside world, [33], ICPT is considered a safer alternative to traditional charging [35]. Because of its high efficiency and safety, ICPT has been increasingly getting notice amongst consumers. However, an increase in distance between the transmitter and receiver, as well as misalignment between the two, has a significant impact on the ICPT's efficiency. ICPT applications include medical implantable devices, fitness bands, EV charging, portable electronic devices electric toothbrushes.

2.4.2 Capacitive Coupling

Capacitive power transfer (CPT) is one of the WPT alternatives that has drawn extensive notice lately because of its low cost. There is no need for heavy magnetic cores, and it has the ability to transfer energy through metal barriers [36]. Both the CPT and ICPT are dominant methods over short-range distances. Conversely, CPT is the ideal approach for charging battery-powered devices because it uses electric field coupling, which is best suited for higher power levels and lower electromagnetic interference. ICPT, on the other hand, has traditionally been used to deal with a wide variety of power loads [37]. Normally, four metal plates are needed to form electric field coupling and deliver a current flow path in a CPT system [37]. Two plates are used as the primary power transmitting unit, and the other two for secondary power receiving unit, causing at least two mutual-coupled capacitors between the four plates. However, the coupling capacitance of current CPT applications is limited by the available space, as is the air gap between the conductors, just like normal capacitors [38]. Moreover, the capacitance is also influenced by the space between the plates. A typical structure of a CPT is shown in Figure 2.5.

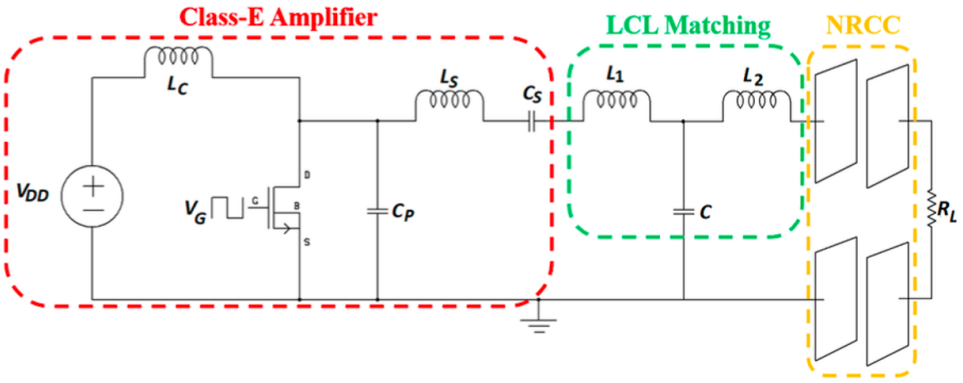

Figure 2.5: Typical structure of a capacitive power transfer system [39].

The key benefit of CPT is that the eddy current losses are negligible [40]. Since an inductive coil is not needed to transmit electricity, eddy current losses only occur on the wires connecting the inverter and charging plates in CPT. The effective frequency at

which power is transmitted between the transmitter and receiver plates in a CPT system is significantly lower than that of an ICPT system.[41]. Higher charging efficiencies can be achieved by adding inductors that adjust the operating frequency and service cycle to compensate for high capacitance. However, CPT systems are easily affected by the misalignment between the plates [41], this may also lead to capacitance variations. Some of the applications of CPT include integrated circuits, medical implantable devices, LED lighting and USB and mobile device charging.

2.4.3 Resonant Inductive Coupling

Resonant inductive coupling (RIC) also known as magnetically coupled resonance (MCR) WPT has gained more attention from the research paradigm. A typical RIC consists of four coils. The basic working principle is such that the transmitting and receiving coils are coupled to resonant coils through inductive coupling by mutual inductance, and the resonant coils achieve wireless power transmission based on electromagnetic effect. Through the resonant state, the transmission loss is reduced due to high impedance performance. Unlike its original system ICPT, which can only achieve high efficiencies at low separation distances, RIC can achieve better transmission efficiencies at longer distances. The frequency band of RIC is usually in the low megahertz. The excitation frequency and the receiver's natural frequency must be in sync for resonance to occur [42]. In fact, selecting the most appropriate resonant frequency for the coil size is critical because in most cases, smaller coils perform better with high frequencies in contrast with the larger coils. Moreover, RIC has the optimum operating distance where optimal efficiency is achieved. In RIC, effective power transfer is enabled by the high quality of the primary and secondary coils [43]. RIC system has the capability to charge multiple devices at the same time, as long as the charged devices are on the area of reach [44]. Also, this involves devices of different power levels and sizes. One of the standards for commercial applications, AirFuel, operates in the 6.78 MHz frequency band. As indicated in Figure 2.6, the main components of the RIC-WPT system are the coupling capacitors. Cou-

pling capacitors are used to tune the transmitting coil as well as the receiving coil to achieve resonance for optimal power transmission efficiency [45]. In order to maintain high transmission efficiency, accurate tuning of resonators is very important throughout the changes in transmission distance to combat the effect of frequency splitting [45]. The method of frequency tuning can mitigate for the variations in frequency as the transmission distance changes. However, this method is often explored more in the experiment phases and not for commercialisation because the frequency ranges should fall within the Industrial, Scientific and Medical (ISM) band [45].

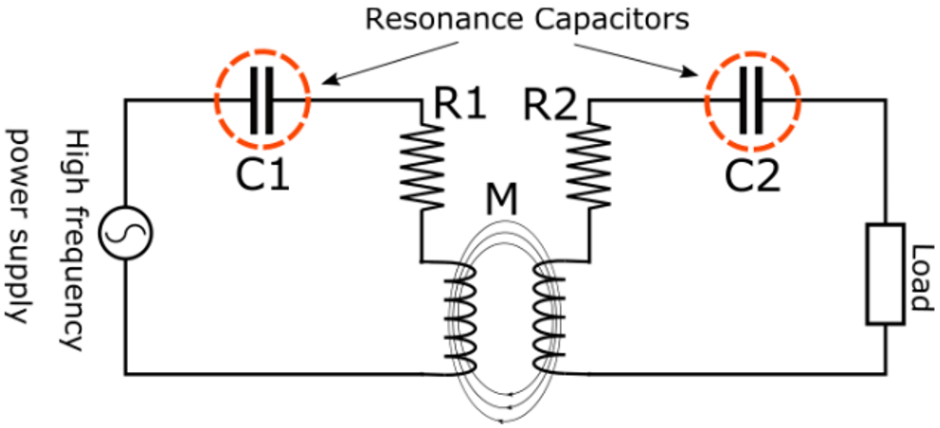

Figure 2.6: Magnetically coupled resonance circuit diagram [7].

The RIC approach differs from ICPT because of its extended transmission ranges. Both the RIC and ICPT are easy to implement and commercialise, however RIC operates at higher frequencies than ICPT [46]. In most WPT systems, safety of the system to the environment is always taken into consideration. RIC offers a safety net because it is non radiant and like most WPT systems, it eliminates the use of power cables [47]. Notwithstanding the convenience of RIC, the size of the system might be a factor to consider. To achieve high efficiencies, high inductance coils may be required, which may increase the size of the whole system [48]. To maintain high efficiency during power transfer, the compensation circuit is required, in order to achieve resonance between the transmitter and receiver, the capacitors in the circuit system must have a low tolerance and be able to compensate for changing mutual inductance between the coils [49]. The

main applications of RIC include medical implantable devices, household applications and EV charging.

2.5 WPT Applications

There are different applications where WPT systems are deployed including in industrial, automotive, aerospace, consumer electronics, medical implantable devices and wireless sensor networks.

2.5.1 Industrial

Wireless power transfer in industrial applications has been growing in the recent years. Current industrial equipment are usually in remote areas and even in spaces where maintenance can be quite a hustle. For example, in harsher environments where there is moisture, hazardous fuels or even dust, transmission cables can be prone to stress which may cause damage and even reduce the lifetime of the cables and the whole situation might contribute to potential risk to human [30]. Not having to continuously replace damaged equipment due to faulty power delivery mechanisms can be of a great boost to the industry. Some of the challenges can be overcome by applications where industrial robots with high special freedom get to be deployed in hazardous environments for efficiency and to spare human workforce [30]. Normally, robots used as a replacement for the workforce require to be charged the entire time, therefore there should be a sort of power storage or receiver like charging pads installed. Low power sensors are often installed together with the charging pad so as to allow the robot to detect when the battery becomes low in order to access the nearest charging station to refill [30]. These sensors usually send the sensed data to the central modules where the captured data can be analysed. The capability of the robots to recharge themselves plays a very important role to minimising human interaction with them as well as workplace injuries. Big factories also install sensors throughout their premises for vast applications. Usually, the sensors

are placed in remote places which can be hardly accessible, such as areas with very low temperature like walk in freezers, areas with high temperatures like ovens, rooftops and wall embedded fire monitoring sensors [50]. Most of these challenges can be overcome by using LPWAN devices to allow for data transmission between machines at a wider area and longer distances to allow for a more reliable industry. Furthermore, WPT charging systems can transform industrial environment immensely.

2.5.2 Automotive

Recent advancements in the automotive industry such as Tesla's mostly waited for long driving range and hard as a rock Cybertruck, a good off roading Rivian's R1T and a pure electric with hydrogen electric Nikola truck, all being zero-emission trucks with electric power as their primary source are a few of most advancements entering the market.To reduce carbon emissions caused by transportation, the number of hybrids and electric vehicles in use has been scaled up and created [51]. However, so far, battery powered vehicles have very short to fair range because eventually batteries run out and need to be recharged. To combat this challenge more companies are putting more effort in research to improve the batterie's lifespan as well as reducing its weight. For this reason, much like LED lights and photovoltaic cells, the prices have dropped considerably in the past years, therefore what was the automotive industry nightmare (high battery prices) have been considerably subsiding. Conversely, lighter batteries will also increase the whole system efficiency of the EV which will be lighter and possibly even faster. The introduction of wireless power transfer charging into the automotive marketplace has proved to boost functionality and portability [52]. Depending on the performance of the charging pad speed and the power of the EV battery, it can take anywhere from 4 to 8 hours to completely charge. In order to realise reliability and efficiency in automotive industry, safety has to be considered top priority. For this reason, electric vehicle manufacturers are making some features standard like, vehicle to vehicle communications, vehicle auto-diagnosis, auto-pilot devices and smart transportation. These safety mechanisms are

achieved by low power sensors which most are part of LPWANs. The application of these sensors and devices unleashes the possibilities to have a wide communication between vehicles and are able to share tons of data from different wide locations. This gives WPT both for the safety sensory devices and for the EV's a high solution consideration. In [53], the authors proposed a system where vehicles are able to charge while driving on a highway. The proposed system will most definitely curb interruptions while changing and save costs. Although, most of the research is being done on electric cars, WPT does also benefit other smaller transportation vehicles including, electric bikes, forklifts, cargo delivery trucks and electric trains just to name a few.

2.5.3 Aerospace

The concept of introduction of solar power satellite (SPS) system in space was studied comprehensively in the 1970s by the U.S. Department of Energy (DOE) and National Aeronautics and Space Administration (NASA) [15]. Most recently, NASA has proposed a new system proving that WPT can work impeccably 1 km above the ground. A solar power exploratory research and technology program was launched by NASA in conjunction with the WPT for commercialisation. Microwave or laser beam would be used to deliver the collected energy that has been gathered from the sun by a satellite which distributes the collected energy to other satellites that are stationed kilometres away from the earth [54]. The use of satellites as the means for WPT charging solution was not the only consideration. The main power for wireless sensor networks (WSN) is batteries, and batteries run out and need to be recharged, and this in most cases limits the ability of the WSN as it has to be in sleep mode most of the time to save energy [55]. To combat the challenge faced when using batteries as the only primary power source for WSN, [56] proposed the use of energy harvesting to supplement the batteries and even for charging. However, energy harvesting depends on the available harvestable energy around the devices environment and the harvested energy is often very little, therefore, WPT charging was proposed in [57]. Moreover, low power wireless sensors are most im-

portant in aerospace as they can be used to assess the landing gear health and fuselage integrity. These devices performance can be boosted by using WPT as their main source of energy, this in turn reduces system weight due to less wiring.

2.5.4 Medicine

Application of WPT for medical implantable devices (IMD) has grown rapidly in the past ten years. Applications such as, implantable nerve stimulators [58], multi-functioning robotic capsules [59] and cochlear implants[39], can without doubt benefit immensely from the use of WPT technology instead of the conventional wires. The use of WPT in medical implantable devices brings satisfaction to patients as well as safety and convenience [60]. Nonetheless, some notable challenges such as negative impact surrounding tissue and wireless signal attenuation have been faced by researchers. It was stressed that wirelessly driven medical devices will also share data with the monitoring system for diagnosis, which will simplify convenience and personalised treatments [61]. Some of the challenges are due to the kind of WPT techniques used. For instance, using radio frequency (RF) as a low power source, where by the device captures the RF power from its surrounding environment, means that there will not be a steady transmission of power since the RF signal fluctuates and this can cause dire situations. The other WPT method used to power IMD is inductive coupling which performs very well in short distances. The only downside to this method is that when the device being charged is misaligned or moves in an area far way from the charger (Transmitter), this may cause excessive heat that might pose a danger to a patient. Safer and less complex WPT techniques need to be presented in order to advance the IMD.

2.5.5 Consumer Electronics

Nowadays convenience is major factor when it comes to portable electronics. Devices like cell phones, laptops, iPods, tablets, smart bands, airpods, etc. have all changed the

way life is and how people live. However, it is notable that most if not all consumer electronics use batteries as their primary power supplies. Batteries are produced in tons yearly and they have a negative impact to the environment [62]. WPT can contribute many advancements including miniaturisation of portable devices and reduced battery sizes or even total elimination of the batteries altogether. While some WPT techniques such as inductive and capacitive can be actively utilised for charging devices, the capacitive charging needs sizeable charging area, or a very high charging frequency [63, 64]. Alternatively, inductive power transfer (IPT) systems have been greatly used for electric toothbrushes [65], sensors [66] and charging pads for mobile phones [67]. It is important to note that a more flexible kind of IPT system which employs resonance, offers extended distances of power transfer and reasonable efficiency. This has caused interest into this kind of IPT technique from industry and research. Also, wearable devices such as smart watches have many sensors which are built in the device. Most of these sensors are low power and operate at certain frequency bands. It is therefore important to consider a WPT technique that can operate at lower frequencies than the charged device.

2.5.6 Wireless Sensor Networks

The advancements in low power sensor networks have been extraordinary in recent years. Low power sensors are often employed for smart city architecture [68], water monitoring [69] and air pollution monitoring [70] just to name a few. These sensors work in a way that they consume very low power because of the way they function. Working together to achieve different tasks, these low power sensor form IoT network. The authors in [71] proposed powering wireless sensor networks with energy harvesting techniques like RF energy. Radio frequency energy harvesting captures energy that is readily available on the devices environment from radio waves. This technique works well since there are radio waves almost everywhere the sensors are situated. However, since this technique depends on radio waves, the harvested energy always fluctuates and this might be a problem. On the other hand, magnetic resonance based energy transfer is selected as a suitable

candidate for charging or even powering low power sensors [72]. Magnetic resonance or strongly coupled resonance WPT is a form of inductive coupling power transfer IPT that uses resonance, both the transmitter coil and receiver coils resonate at the same frequency allowing for extended distances in power transmission with good efficiency.

2.6 WPT Standards

2.6.1 Qi Charging standard

In order to have viable WPT charging systems which are safe and market ready, certain standards need to be taken into consideration. The Qi standard of charging was founded by Wireless Power Consortium (WPC), built in collaboration by world largest manufacturers from wide range of industries [17]. This standard standardises concerns for WPT systems and lists, but not restricted to, interoperable wireless charging formats, power requirement categories and alignment approaches [72, 17]. WPT systems and circuits adhering to this standard are proposed in [73, 74]. The history, viewpoint and specifications for the Qi standard is presented in [17].

2.6.2 Air-Fuel Alliance standard

Air-Fuel Alliance WPT standard by Alliance for Wireless Power (A4WP) was introduced in 2012. Initially it was called Rezence WPT standard which changed because of the merge with Power Matters Alliance [7]. This standard operates at 6.78 MHz and uses magnetically coupling scheme [75]. Some of the WPT systems and circuit topologies employing this standard are described in[76].

These WPT standard are used to regulate and standardise different charging solutions that are proposed and on the works. In this work, 40.68 MHz of industrial, scientific and medical (ISM) band that is widely used for radio frequency identification (RFID) under

the Qi standard is considered.

2.7 WPT for Small Sensor Devices

Nowadays it is more convenient and efficient to use WPT for small electronics, wireless sensor networks (WSN), low power wide area networks, household applications, etc. Wireless power transfer is considered much safer and applicable to very remote areas. Since its introduction in the 1800s, there have been numerous developments and optimisations of WPT systems from the research paradigm and industry. In this chapter, some of the most common system considerations and developments in order to maximise the efficiency of WPT system are discussed. Our focus is based more on resonant inductive coupling or strongly coupled magnetic resonance WPT as per the focus of this research.

2.7.1 WPT using SCMR for Low Power Wide Area Network (LPWAN)

LPWAN refers to a sort of wireless communication technologies that offer long data transmission ranges, low power consumption rates, low development cost of the device, high scalability and long battery lifetime [68]. Considering the supply of power for smart sensors, as mentioned, the use of batteries becomes a primary solution. Although some batteries are made to last longer, some challenges with this method can be maintenance (battery replacement) and environmental impact (battery ecotoxicity)[77]. Energy harvesting, where energy is harvested around the devices' environment to recharge the storage element, was proposed as a viable solution [78]. However, realising a balance between the inconsistent harvested power and consumed power in such a system while keeping sufficient quality of service (QoS) is a challenging task [79]. Hence, WPT has emerged to be a viable alternative in inaccessible spaces, typically places where it is hard to reach [80]. Magnetically coupled resonance or strongly coupled magnetic resonance WPT becomes the most suitable choice to power these systems. SCMR-WPT can transfer power from

centimetres to few meters at a reasonable efficiency. It operates at different frequency band (typically 6.78 MHz, 13.56 MHz and 40.68 MHz for fixed and mobile services) than LPWAN data transmission range (typically 433 MHz and 915 MHz) and there is low interference from surrounding objects. Also, in an SCMR-WPT, power can be transmitted through obstacles such as walls, water, glass and other non-conductive materials.

SCMR-WPT systems usually have four coils. The use of four coils is to compensate for coupling coefficient variations which in turn contribute to extended power transmission distances and therefore high transmission efficiency. In this system, there is an optimal range, where transmission efficiency is at maximum. However, distances beyond this range will contribute to sharp decline in transmission efficiency. This is caused by impedance mismatch which also affect the resonant frequency. Ranges below this optimal range also contribute to decrease in efficiency and this is due to frequency splitting. In order to address these issues a frequency tracking method was proposed in [81]. This technique tracks the frequency and matches the whole system frequency so that the transmitting and receiving coils resonate, thus maintaining high transmission efficiency. However, the frequency tracking method is not suitable for commercialisation because the matched frequencies often fall outside the ISM band. Impedance matching is another method to overcome the aforementioned challenges [82]. In this technique, the input impedance is matched with the load impedance. Although impedance matching is more viable because the resonant frequency of the system is maintained, it requires additional control circuits, which might be bulky and difficult to implement. Authors in [83], proposed a reconfigurable coil to mitigate for misalignment, frequency splitting and coupling coefficient variations. The system works in such a way that the coils are adjusted as the distance changes to mitigate for the changing coupling coefficient, which is crucial for an efficient SCMR-WPT.

In our study, SCMR-WPT is considered for powering LPWAN devices. Wireless power

is very necessary especially in applications like Structural Health Monitoring (SHM). Most SHM devices are LPWAN, this has an added advantage to the application as low power sensors such as LoRa, which falls within LPWAN devices, can wirelessly transmit data in long distances typically 15 km. Also, in mega structures like bridges all the parts of the structure my not be accessible for observation, making the use of LPWAN powered wirelessly for SHM a safer and more practical solution. Based on the above mentioned considerations, this study will focus on the design and optimisation of an efficient wireless power transfer system based on existing systems. More efficient methods and implementations will be followed in order to address some bottlenecks in the WPT research such as bulkiness of the system, complexity of the system and low transmission efficiency challenge.

2.8 Summary

In this chapter, the history of WPT was discussed, followed by WPT techniques which include radiative WPT, laser and microwaves, non-radiative, inductive, capacitive and resonant inductive. Advantages and disadvantages of these techniques were also provided. These were followed by WPT applications which included industrial, automotive, aerospace, medicine, consumer electronics and wireless sensor networks and low power wide area networks. WPT standards were also outlined consisting of Qi standards and Air-fuel Alliance standard. The use of WPT for small electronics was thoroughly stipulated, focusing on WPT using SCMR for LPWANs.

Chapter 3

Modelling and Design of WPT via SCMR

In this chapter, optimal design for conformal SCMR (CSCMR) WPT is investigated. The use of the equivalent circuit model together with the derived formulae are used to make analysis. An SCMR-WPT can be represented as an RLC circuit for analysis. Therefore, section 3.1 presents the equivalent circuit model and mathematical analysis thereof. A systematic derivation of an optimal resonator loop is discussed in section 3.2, whereby specific physical and electrical parameters are observed and generated with the most efficient and non-computational intense method using MATLAB. The generated data is then reviewed. Section 3.3 then discusses the Capacitor-loaded and Self-resonant CSCMR-WPT systems and compares their transmission efficiencies.

3.1 Four-Loop Model Analysis

A conventional WPT method using strongly coupled magnetic resonance (SCMR) comprises of four coils of which two acts as the source loop and the load loop, while the other two are resonators (Tx loop and Rx loop) as shown in Figure 3.1. SCMR system works in such a way that the source loop is inductively coupled with the Tx loop, and likewise, the

load loop follows the same sequence with the Rx loop [84, 85]. The resonator loops are designed to operate at the frequency where their quality factor (Q) is at its maximum, the chosen frequency of operation must coincide with this frequency. The advantage of having the Tx loop and the Rx loop operating at specified resonant frequency ensures strong energy coupling and makes the system less prone to other resonating material around it. This also ensures efficient power transfer between the source/load loops.

In the system shown in Figure 3.1, $d1$ is the spacing between the source loop and the Tx loop, $d2$ is the spacing between the Tx and Rx loops and d3 is the spacing between Rx loop and load loop. A typical SCMR system has an optimum spacing for $d1$ and $d3$ where the efficiency is maximum [86]. Actually, any spacing $d1$ and $d3$ beyond these optimum values will result in efficiency decrease. Taking these factors into consideration, it is clear that for the SCMR system to optimally transmit power, it should have certain dimensions as shown in Figure 3.1, which can be bulky when the system is being utilised for small devices/applications. Therefore, conventional SCMR systems can occupy large volume and this can make it difficult to incorporate the system into various applications such as, wearable monitoring devices and biomedical implants.

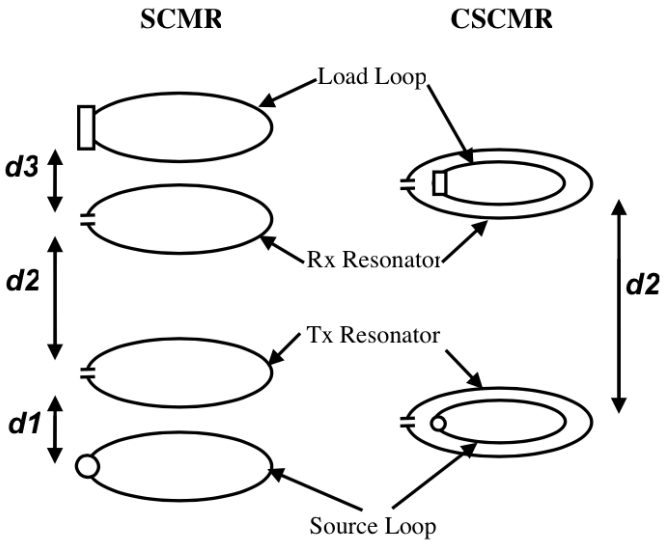

Figure 3.1: SCMR and CSCMR comparison

In order to overcome the bulkiness of SCMR, Conformal SCMR (CSCMR) was previously studied in [87, 88]. Figure 3.1 shows the layout of CSCMR next to the SCMR, where the source and the load loop fit concentrically inside the Tx and Rx loops. This method revolutionises the SCMR as the spacing $d1$ and $d3$ are completely eliminated, therefore making the system smaller. A conventional conformal SCMR (CSCMR) system based on loops depicted in figure 3.1 can be represented in an equivalent RLC circuit shown in Figure 3.2. Loops are often preferred in CSCMR because of their small footprint and easy to fabricate nature.

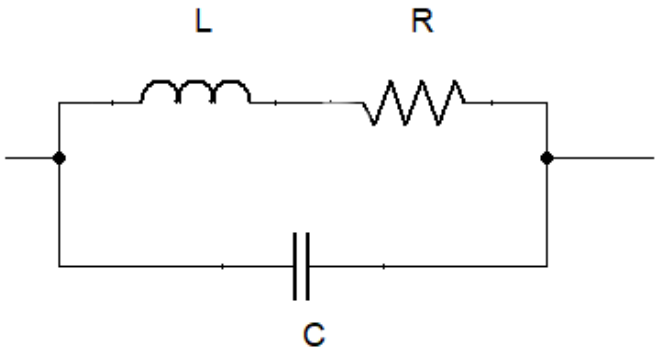

Figure 3.2: The RLC representation of the resonator loop.

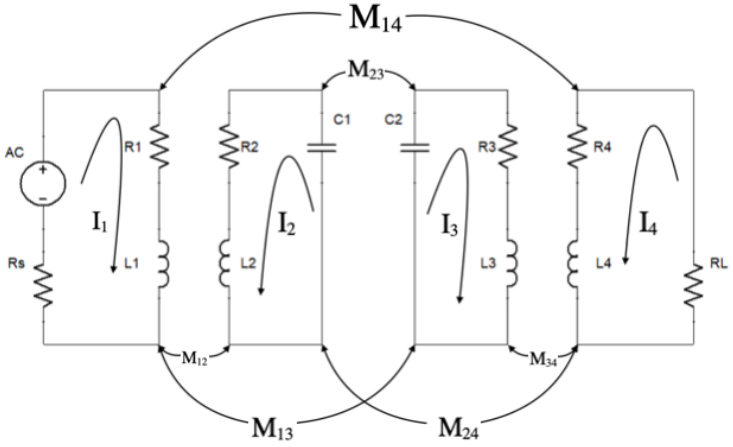

Figure 3.3: Equivalent circuit model of SCMR and CSCMR

An equivalent circuit model of the four loop CSCMR system with one pair resonators, a source loop and load loop is derived as depicted in Figure 3.3. All mutual inductances are taken into account in this system. Based on the circuit model shown in Figure 3.3,

using Kirchhoff's Voltage Law (KVL) for a four-port network analysis, the equivalent circuit model can be described by the formulas given below [89, 90]:

$$\begin{aligned} V_S &= (R_S + R_1 + jwL_1) * I_1 + jwM_{12} + jwM_{13} * I_3 + jwM_{14} * I_4 \\ 0 &= jwM_{21} * I_1 + (R_2 + jwL_2 - j/wC_1) * I_2 + jwM_{23} * I_3 + jwM_{24} * I_4 \\ 0 &= jwM_{31} * I_1 + jwM_{32} * I_2 + (R_3 + jwL_3 - j/wC_2) * I_3 + jwM_{34} * I_4 \\ 0 &= jwM_{41} * I_1 + jwM_{42} * I_2 + jwM_{43} * I_3 + (R_L + R_4 + jwL_4) * I_4 \end{aligned} \tag{3.1}$$

The equivalent circuit equations (3.1) can be converted to matrix in terms of current as follows:

$$\begin{bmatrix} I_1 \\ I_2 \\ I_3 \\ I_4 \end{bmatrix} = \begin{bmatrix} Z_{11} & Z_{12} & Z_{13} & Z_{14} \\ Z_{21} & Z_{22} & Z_{23} & Z_{24} \\ Z_{31} & Z_{32} & Z_{33} & Z_{34} \\ Z_{41} & Z_{42} & Z_{43} & Z_{44} \end{bmatrix}^{-1} \begin{bmatrix} V_S \\ 0 \\ 0 \\ 0 \end{bmatrix} \tag{3.2}$$

Where:

$$\begin{Bmatrix} Z_{ij} = jwM_{ij} \ (i \neq j) \\ Z_{11} = R_S + R_1 + jwL_1 \\ Z_{22} = R_2 + jwL_2 - j/wC_1 \\ Z_{33} = R_3 + jwL_3 - j/wC_2 \\ Z_{44} = R_L + R_4 + jwL_4 \end{Bmatrix} \tag{3.3}$$

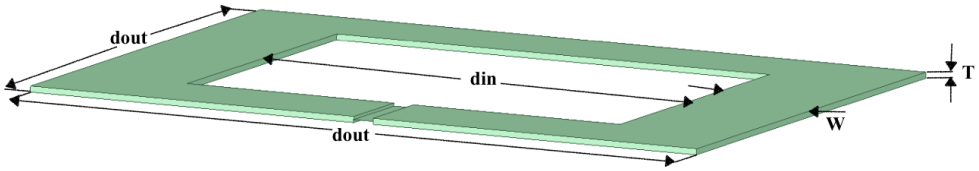

Figure 3.4: Loop model geometry.

A rectangular cross-section of a square loop is shown in Figure 3.4. The basic dimensional parameters of the loop are thickness (T), width (W), inner diameter (d_{in}) and the outermost diameter of the loop (d_{out}) respectively. The inner diameter d_{in}, can be derived from the other geometrical parameters as:

$$d_{in} = d_{out} - 2(W) \tag{3.4}$$

Where r_{outer} is the outer diameter of the loop and W is the width of the loop. The total length l_{tot} of the spiral can be calculated as:

$$l_{tot} = 4d_{out} \tag{3.5}$$

According to (3.6), the self-inductance of the square spiral loop [91] can be calculated as:

$$L = \frac{x_1 \mu_0 r_{avg}}{2}\left[ln\frac{x_2}{r_d} + x_3 r_d + x_4 r_d^2\right] \tag{3.6}$$

$$r_d = \frac{d_{out} - d_{in}}{d_{out} + d_{in}} \tag{3.7}$$

Where $x_1 = 1.27, x_2 = 2.07, x_3 = 0.18, x_4 = 0,13, \mu_0$ is the permeability of free space, $r_{avg} = (d_{out} + d_{in})/2$ and r_d is the fill factor. The ohmic and radiation resistance of a spiral loop can be written as [92, 93, 94]:

$$R_{ohm} = \frac{l_{tot}}{4\sqrt{WT}}\sqrt{\pi \mu_0 p f} \tag{3.8}$$

$$R_{rad} = 31200\left(\frac{f}{c}\right)^4\left(\sum_{i=1}^{n} l_i^2\right)^2 \tag{3.9}$$

Where l_i is the side length of the i_{th} turn of the spiral, c is the speed of light, T is the thickness of the conductive trace, n is the number of turns in the case of a coil and p is the spiral's conductor resistivity [93]. The effective resistance of the spiral can be given as:

$$R_{eff} = R_{ohm} + R_{rad} \tag{3.10}$$

For a more precise calculation of the mutual inductance between two loops, a simplified Neumann's equation expanded up to the 30th order can be expressed as [95]:

$$M = \left(\frac{4}{\pi}\right) \sum_{n=i}^{i=n_1} \sum_{n=j}^{j=n_2} M_{ij} \tag{3.11}$$

$$M_{ij} = \frac{\mu_0 \pi a_i^2 b_j^2}{2\left(a_i^2+b_j^2+d^2\right)^{2/3}} \left(1 + \frac{15}{32}\gamma_{ij}^2 + \frac{315}{1024}\gamma_{ij}^4 + \frac{15015}{65536}\gamma_{ij}^6 + ... + 0.6028\gamma_{ij}^{28}\right)$$

$$\begin{aligned} a_i &= r_{o1} - \tfrac{W_1}{2} \\ b_j &= r_{o2} - \tfrac{W_2}{2} \\ \gamma_{ij} &= \tfrac{2a_i b_j}{a_i^2+b_j^2+d^2} \end{aligned} \tag{3.12}$$

Where d is the distance between two spiral loops and r_{o1} and r_{o2} are outer radii of the spiral loops.The equivalent circuit model presented in Figure 3.3 can have a mathematical solution derived as:

$$[I] = [V]/[Z] \tag{3.13}$$

Thus, the transfer efficiency can be acquired from the scattering parameter S_{21}, which denotes the injected signal at the input and the signal at the output port. The ratio between the voltage obtained at the load and the source (V_{load}/V_{source}) can be calculated first and the expression of transfer efficiency will then be:

$$\eta = |S_{21}|^2 = \frac{V_{load}^2/R_{load}}{V_{source}/4R_{source}} \tag{3.14}$$

Where both R_{source} and R_{load} are assumed to be 50Ω. The voltage at the load can be written as:

$$V_L = (-I_4)R_L \tag{3.15}$$

Based on equations (3.12) and (3.13), the efficiency can be derived as:

$$\eta = |S_{21}|^2 = \frac{4w^6 M_{21}^2 M_{32}^2 M_{43}^2 R_1 R_4}{(A+B+C+D+E)^2} \tag{3.16}$$

$$\left\{ \begin{array}{c} A = Z_{11}Z_{22}Z_{33}Z_{44} \\ B = M_{12}M_{21}Z_{33}Z_{44}w^2 \\ C = M_{23}M_{32}Z_{11}Z_{44}w^2 \\ D = M_{34}M_{43}Z_{11}Z_{22}w^2 \\ E = M_{12}M_{21}M_{34}M_{43} * w^4 \end{array} \right\} \tag{3.17}$$

The CSCMR system will have maximum efficiency when working at resonance, the resonant frequency can be determined as:

$$f_r = \frac{1}{2\pi\sqrt{LC}} \tag{3.18}$$

It is also required that the resonators have high Q-factor for the system to be efficient[96], Q factor of a spiral loop can be expressed as follows:

$$Q_i = \frac{2\pi f_r L_i}{R_i} \tag{3.19}$$

The coupling coefficient between two loops can be derived as:

$$k_{ij} = \frac{M_{ij}}{\sqrt{L_i L_j}} \tag{3.20}$$

Taking (3.19) and (3.20), efficiency can be derived by substituting the Q-factor and the coupling coefficient to get:

$$\eta = \frac{4k_{21}^2 k_{32}^2 k_{43}^2 Q_2^2 Q_3^2 Q_1 Q_4}{(1 + k_{12}k_{21}Q_1Q_2 + k_{23}k_{32}Q_2Q_3 + k_{34}k_{43}Q_3Q_4 + k_{12}k_{21}k_{34}k_{43}Q_1Q_2Q_3Q_4)^2} \tag{3.21}$$

In CSCMR systems, it is very critical that the resonators are designed in a way that they resonate at the resonant frequency which coincides with the frequency where the resonators naturally have high Q-factor. This in turn ensures maximum transmission efficiency.

3.2 Optimal Resonator Loop Derivation

To transfer power efficiently, highly resonant systems that operate in a strongly-coupled regime are required. These systems are more efficient when compared to their non-resonant counterparts. Since highly resonant systems work efficiently under certain frequencies, careful consideration of the systems geometry is required when calculating the resonant frequency. To achieve this, in this section, equations are derived and used to calculate optimal electrical characteristics which are then used to determine the resonant frequency and Q-factor of the loops. From the efficiency calculations, it will also be clear that Q-factor needs to be maximised to yield optimal transmission efficiency. Then the equation for maximum Q-factor will be derived which will be used to re-assess the physical dimensions of the WPT system to maximise transmission efficiency. The following parameters of the loop are considered:

- Capacitance, C (for capacitor loaded resonator)

- Self-inductance, L
- Resonant Frequency, f_r
- Loss impedance, Γ
- Quality factor, Q

The above-mentioned parameters are directly related to the physical dimensional parameters of the loop under consideration, as well as the properties of the loop material (Copper).

- Thickness of the of the wire, T
- Radius of the loop, $d_{out}/2$
- Width, W
- Height, h (for 2-layer self-resonant resonator)

In order to attain optimal transmission efficiency, CSCMR-WPT system has to resonate where the resonators attain maximum Q-factor. This phenomenon can also be observed in a simplified equation from (3.21). Since the Tx and Rx resonators need to resonate at the same resonant frequency, their physical dimensions are chosen to be similar in this work. This also makes it easy for the resonators to exhibit the same Q-factor. Therefore $Q_2 = Q_3 = Q$, (3.21) can be rewritten as:

$$\eta = \frac{4k_{21}^2 k_{32}^2 k_{43}^2 Q^4 Q_1 Q_4}{(1 + k_{12}k_{21}Q_1Q_2 + k_{23}k_{32}Q^2 + k_{34}k_{43}QQ_4 + k_{12}k_{21}k_{34}k_{43}Q_1Q^2Q_4)^2} \tag{3.22}$$

From equation (3.22) it can be clearly seen that the Q-factor needs to be maximised in order to maximise the transmission efficiency. Since the Q-factor is the function of f_r, the maximum frequency which will coincide with the maximum Q-factor needs to be

determined as well. The Q-factor and the derived f_{max} using standard calculus are given as:

$$Q = \frac{2\pi f_0}{2\Gamma} \tag{3.23}$$

$$\Gamma = \frac{R_{eff}}{2L} \tag{3.24}$$

$$f_{max} = 120.44 * 10^6 \left[\frac{l_{tot}\sqrt{\pi\mu_0}}{\sqrt{WT}\,(\sum_{i=1}^{n} l_i^2)^2} \right]^{2/7} \tag{3.25}$$

Where Γ is the loss impedance of the loop which is a function of R_{ohm} and R_{rad}. The maximum Q-factor can also be derived using standard calculus to get equation (3.26):

$$Q_{max} = \frac{2\pi f_{max} \frac{x_1\mu_0 \frac{2W}{2d_{out}-2W}}{2} \left[ln\frac{x_2}{\frac{2W}{2d_{out}-2W}} + x_3\frac{2W}{2d_{out}-2W} + x_4(\frac{2W}{2d_{out}-2W})^2 \right]}{\frac{l_{tot}}{4\sqrt{WT}}\sqrt{\pi\mu_0 p f_{max}} + 31200\left(\frac{f_{max}}{c}\right)^4 (\sum_{i=1}^{n} l_i^2)^2} \tag{3.26}$$

3.2.1 Implementation and Analysis

The mathematical equations examined are implemented in MATLAB. Figure shows a MATLAB flow digram for this design. In the implementation, the function involves the geometric parameters of the loop and in turn specifies the resonant frequency (f_r), self-inductance (L), capacitance (C), Q-factor and other characteristics of the loop. Through system level implementation, in this section, the MATLAB model block diagram will be discussed. Figure 3.5 describes the overall implementation procedure of the mathematical model and all the dependencies among characteristics. Geometric parameters discussed earlier are used as inputs, then the self-inductance and the capacitance are calculated. The use of MATLAB code to determine the optimal resonator loop come with a number of advantages in that the computational time is reduced significantly, the computational resources are less, and accuracy to the theoretical analysis is good compared to the 3D simulating software [97]. This in turn makes it possible for the resonant frequency to be

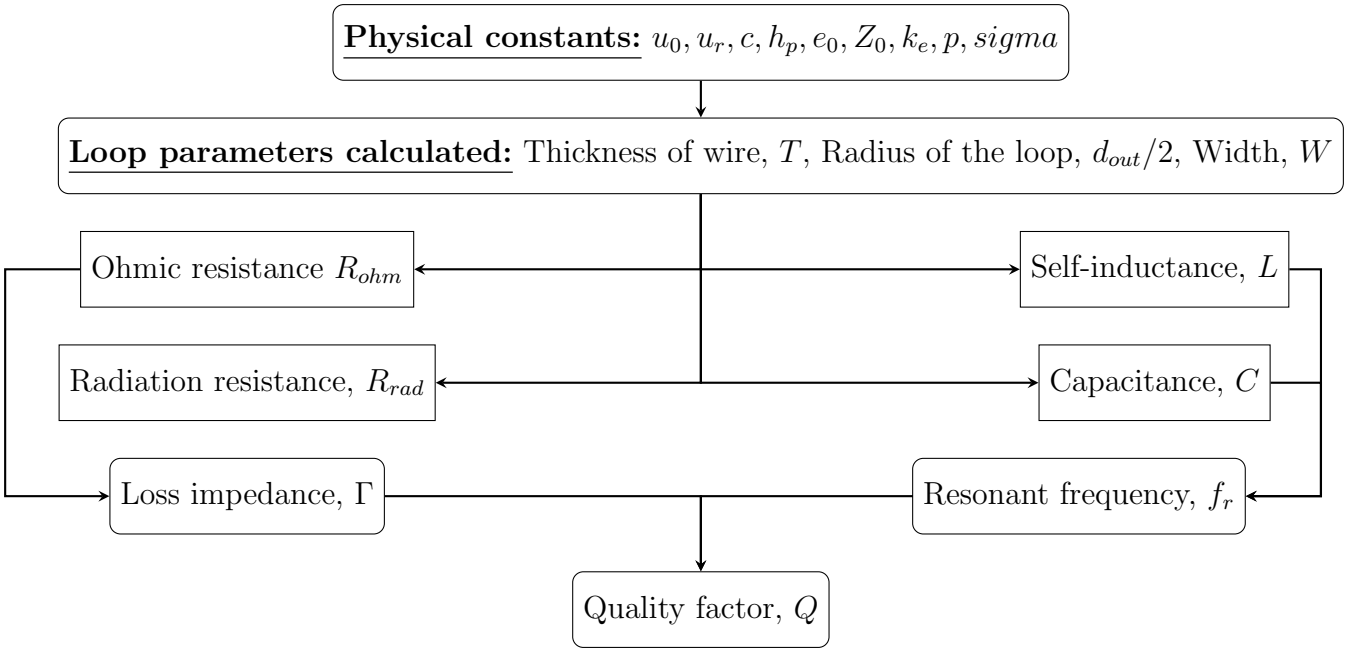

Figure 3.5: MATLAB model flow diagram.

calculated. All the calculated values are then printed out in the command window for evaluation and analysis.

3.2.2 Analysis

The design model that is under investigation by the authors has to be suitable for small low power sensors which have small footprint. Therefore, the physical dimensions of the WPT system have to follow the same notion. In this work, the model is restricted to 100 mm dimension, this means that the resonator's outermost diameter can not exceed 100 mm. This consideration was informed by [98, 99], where LoRa low power networks are used for structural health monitoring (SHM). The default values of the geometry are provided in Table 3.1.

Table 3.1: Default values fed into MATLAB for the geometry

Parameters	Default values
T (mm)	0.05
W (mm)	10
d_{out} (mm)	100

Varying width, W

Since this section focuses on the loop, the resonator loops have a capacitor connected so as to resonate the WPT system at a required resonant frequency. For this reason, a $72pF$ capacitor was substituted in (3.18) so that the effects of width can be observed on the resonant frequency. From the self-inductance (L) formula, it can be seen that increasing in width W results in increasing L, and this influence in turn results in the decrease in resonant frequency (f_r). Now, since f_r and L are the function of quality factor (Q), the combination of these two parameters with increasing W results in the increasing Q. The width is varied from 2mm to 12mm.

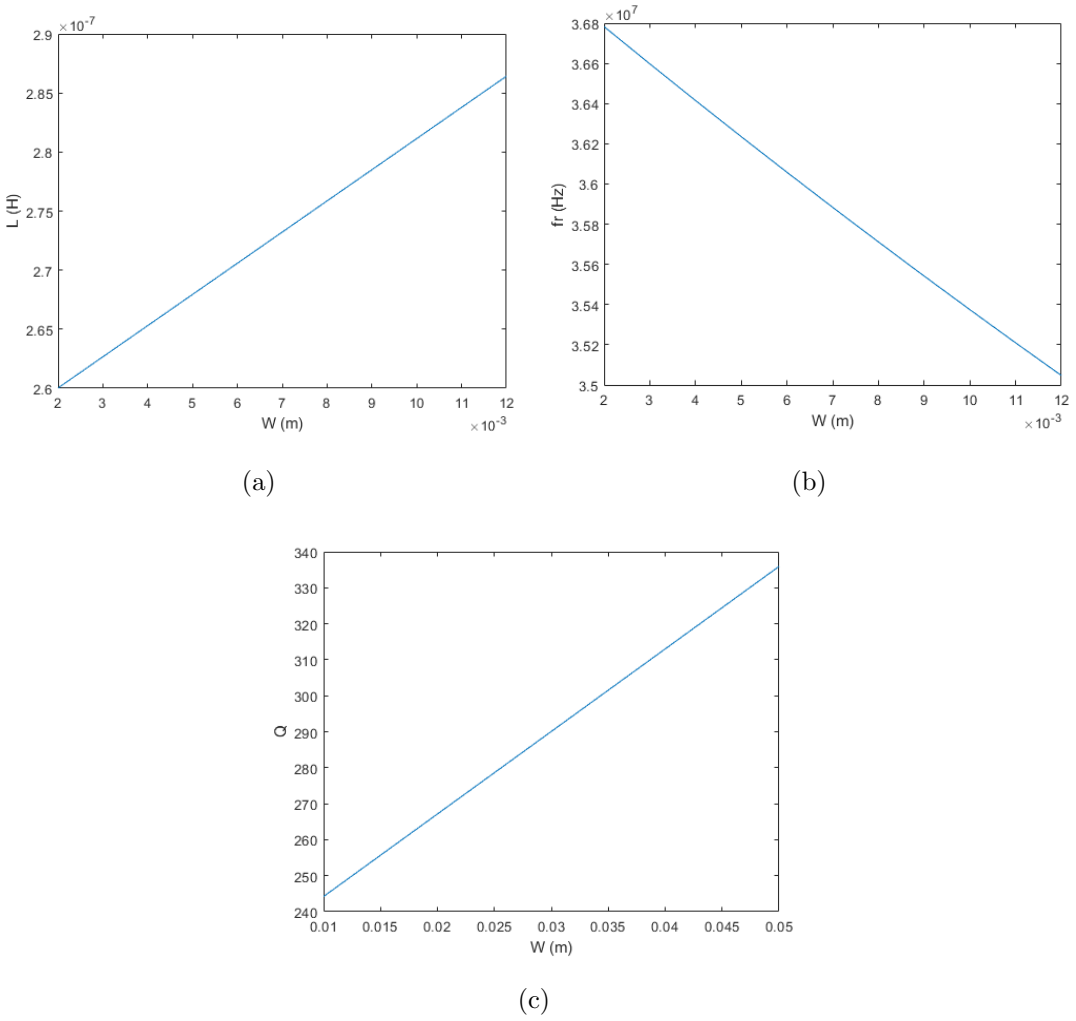

Figure 3.6: Varying the width, W and the corresponding influence on (a) L, (b) f_r and (c) Q.

Varying the outermost diameter, d_{out}

Increasing the outermost diameter of the loop means increasing the overall dimensions of the WPT system. In this work the physical dimensions of the whole WPT system are restricted to 100 mm which means the highest outermost diameter of the loop (resonator) can be 100 mm. From equations (3.6) and (3.10), the influence of d_{out} can be observed and it is clear that the increase in d_{out} results in the increase in L and decrease in f_r. It can also be observed from the formulae that Q increases because of this variation. The outermost diameter of the resonator (loop) is varied from 50 mm to 100 mm.

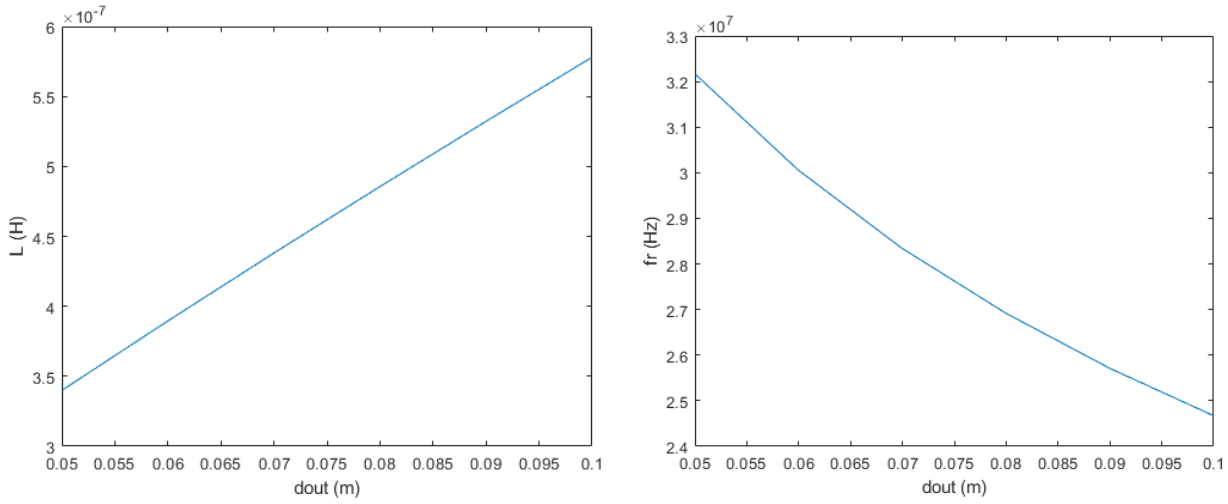

(a) (b)

Figure 3.7: Varying the outermost diameter, d_{out} and the corresponding influence on (a) L and (b) f_r.

Varying thickness, T

Varying the thickness has shown to have noticeable influence on the Q-factor. When T increases the quality factor also sees an increase. This relationship shows to have limits, as more and more increase in T does not necessarily mean direct increase in the Q-factor as observed in the Figure 3.8 below. Thickness does not have any influence on the self-inductance as well as the resonant frequency. The variation of T goes from 0.02 mm to 0.1 mm.

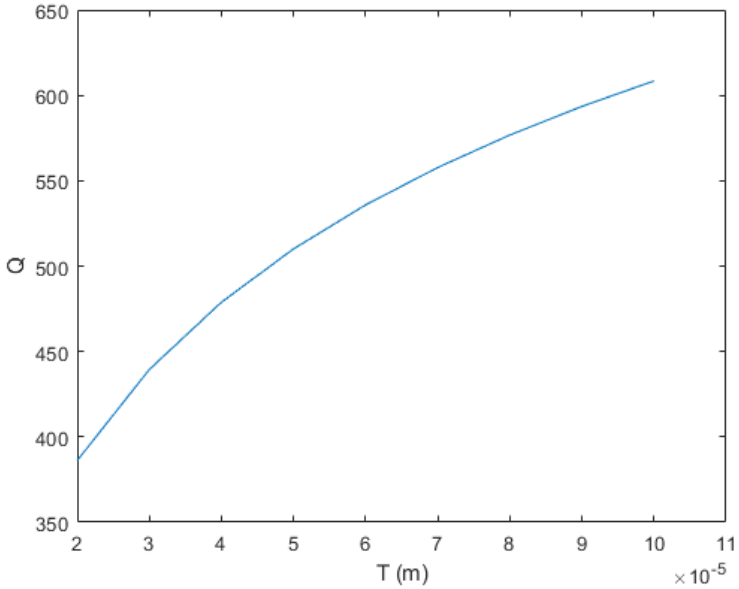

Figure 3.8: Varying thickness, T.

MATLAB generated results (parameters)

These results were generated from MATLAB code consisting of functions which included equations (3.6, 3.8, 3.9, 3.18, 3.19, 3.20, 3.22, 3.23, 3.24, 3.25 and 3.26) from sections 3.1 and 3.2. The results were printed on the command window.

Design – Copper Loop (resonator)

Outermost diameter	= 95.50960 mm
Width	= 5.68990 mm
Thickness	= 0.02990 mm
Length of wire (loop)	= 382.03860 mm
Estimated L	= 0.28250 uH
Estimated Q	= 427.45777
Calculated resonant frequency:	60 MHz
True resonant frequency:	59 MHz

Design – Copper Loop (source/load)

Outermost diameter	= 59.74010 mm
Width	= 5.68990 mm
Thickness	= 0.02990 mm
Length of wire (loop)	= 238.96040 mm
Estimated L	= 0.15430 uH
Estimated Q	= 504.23660
Calculated resonant frequency:	81 MHz
True resonant frequency:	78 MHz

In order to validate and study further, the capability of the generated resonator loop, the generated parameters are used to build a 3D model in high frequency structure simulator (HFSS). In this process, the resonator will be first simulated with the given dimensions from MATLAB in order to extract the simulated self-inductance and the Q-factor. Then, the resonators and source/load loops are combined to achieve a complete CSCMR-WPT system. Next, a two-layer resonator (self-resonant) is compared with the conventional MATLAB derived (capacitor-loaded) CSCMR-WPT system.

3.3 Capacitor-loaded and self-resonant CSCMR-WPT systems

In this section, a self-resonant CSCMR-WPT system which includes the distributed inductance and capacitance is studied. In this kind of configuration, no lumped components are required since the system can achieve large capacitance or inductance. This also becomes beneficial as the complexity of the whole system is lessened as well as the cost involved. Figure 3.9 depicts an equivalent circuit model for a typical self-resonant resonator. As shown in the circuit, the two layers will result in the increase in inductance

which is the sum of $L_s + L_p$. Large parallel-plate capacitance $C_p + C_s$ means an increase in capacitance as well.

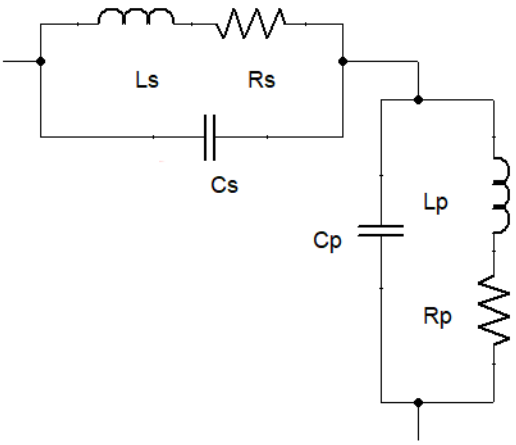

Figure 3.9: A two-layer resonator with self-capacitance

A self-resonant CSCMR-WPT simulation is built (Figure 3.10) based on the equivalent circuit model. The self-resonant system proposed by the authors has some advantages in that the system does not require lumped capacitors which makes the system less complex and easy to fabricate, and the self-resonant system can be tuned to operate at lower frequency bands, i.e., 40.68 MHz ISM without sacrificing too much of transmission efficiency. In order to compare the performance of a self-resonant with the MATLAB derived conventional capacitor-loaded CSCMR-WPT system, the physical parameters of the self-resonant CSCMR are chosen to be the same as the capacitor-loaded system (the above results for a copper loop (resonator)) and the initial height is chosen to be small to adhere to the small footprint of the design: $d_{out} = 95.5mm$, $h = 0.37mm$, $W = 6mm$ and $T = 0.03mm$. The height (h) is fine tuned in HFSS to resonate the resonators as well the whole WPT system at the required resonant frequency.

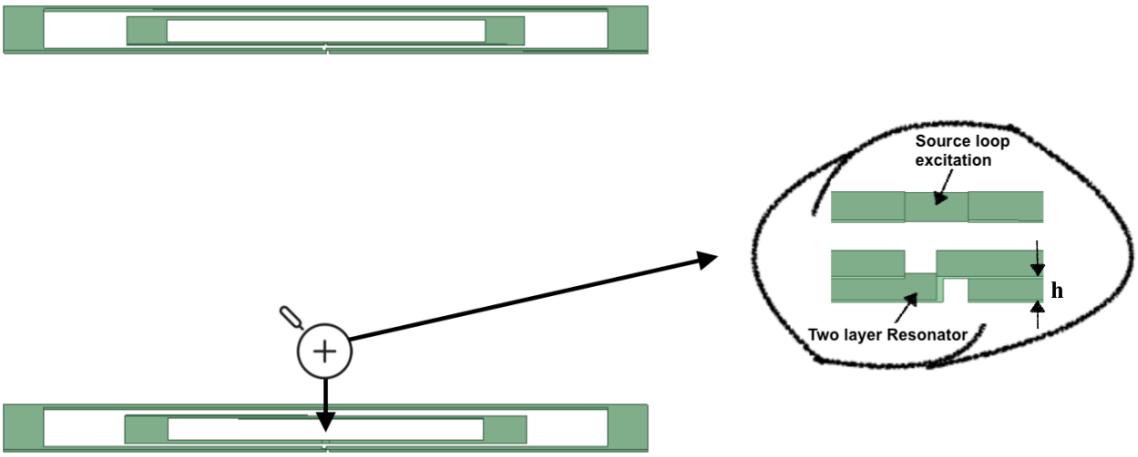

Figure 3.10: A self-resonant CSCMR-WPT system.

The performed simulations compared results for a conventional capacitor-loaded and self-resonant CSCMR-WPT systems with the same physical parameters with the self-resonant system having two layers (Figure 3.11). It is evident that the self-resonant in this case, with the given dimensions, has a higher transmission efficiency than that of conventional model while still maintaining a small footprint. External capacitors also have losses, which can reduce the Q-factor of the Tx and Rx components, lowering the transmission efficiency of CSCMR systems. The self-resonant CSCMR-WPT system can also be tuned to work at the appropriate frequency while taking into account the maximum quality factor of the resonator.

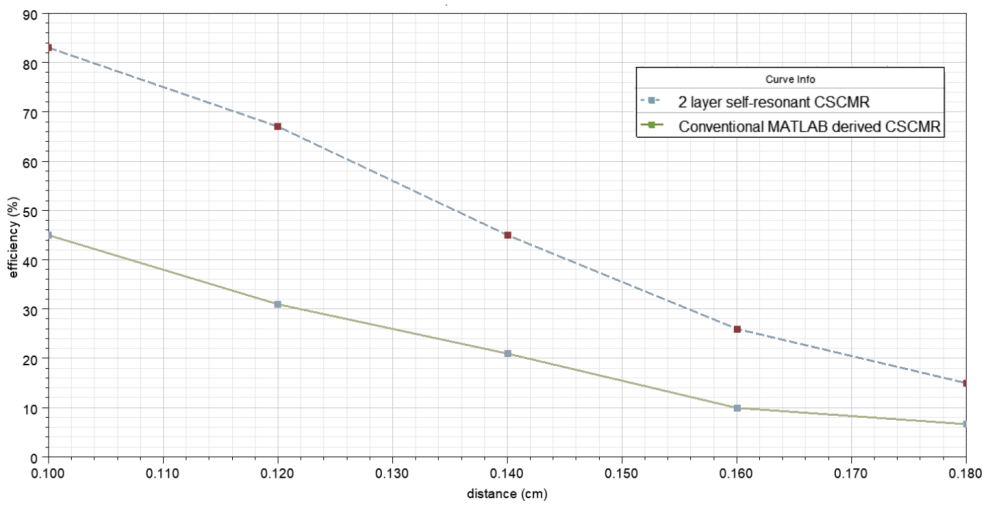

Figure 3.11: Comparison of the conventional MATLAB derived CSCMR-WPT system with the proposed 2-layer self-resonant model.

In Figure 3.11, the MATLAB derived and the 2-layer CSCMR-WPT systems are depicted. It is worth noting that from the MATLAB derived parameters, a conventional CSCMR-WPT system was realised and then updated so that it can self-resonant, hence an added layer making a 2-layer CSCMR-WPT. From the presented data, it can be seen that the MATLAB derived system is not far away from other conventional models. The transmission efficiency at 100 mm, which is slightly above the systems' maximum point of transmission which coincides with the systems' outermost diameter which in this case is 95.5 mm, therefore the maximum attainable transmission efficiency of 46% shown in Figure 3.11 makes more sense [100, 101, 102]. The 2-layer resonator realised from the same dimensions from MATLAB derivation has a higher efficiency of 82.5% at 100 mm. A number of factors contribute to this result which include the self-inductance (L) and the mutual inductance (M). From Figure 3.11, it is clear that when the number of layers is increased, so is the self-inductance, and this results in the increase in mutual inductance between the loops. This increase means that the coupling coefficient (k) between the loops becomes stronger and therefore more power can be transferred effectively. This notion then explains the higher transmission efficiency of a 2-layer CSCMR-WPT system having an efficiency of 83% at 100 mm while keeping a small footprint with the resonator loops being the same dimensions as the MATLAB derived loops. The next chapter presents a co-simulation between HFSS and OptiSLang. Figure 3.12 shows a systematic method used in this work for the optimisation of CSCMR-WPT.

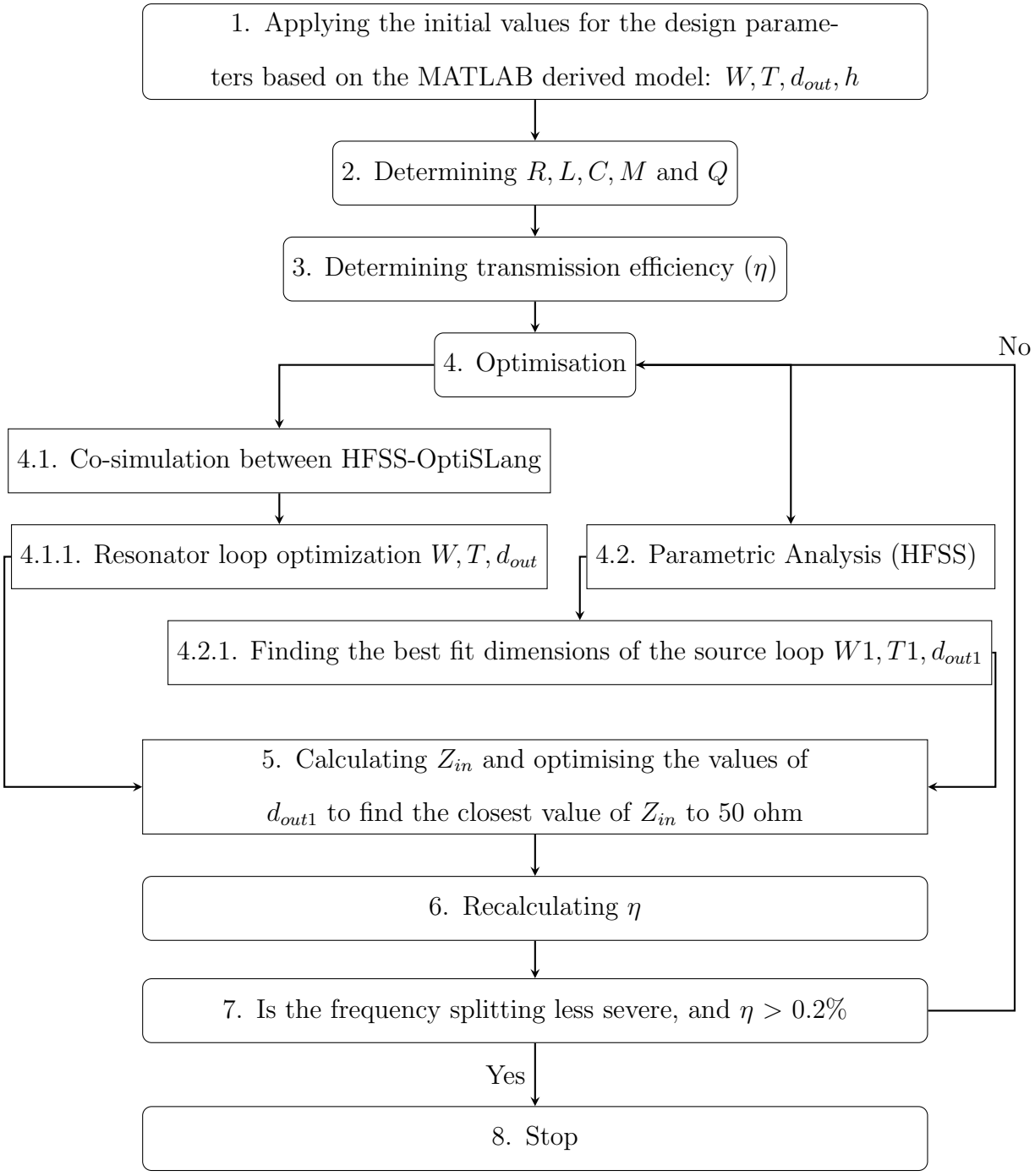

Figure 3.12: CSCMR design optimisation flowchart.

3.4 Summary

In this chapter, equivalent circuit models were used for mathematical analysis. The mathematical analysis help in evaluating different physical and electrical parameters of a wireless power transfer system and make it possible to see what influence one parameter has on the whole WPT system. These derived mathematical formulae were then applied in MATLAB with some functions in order to yield an optimal resonator loop which is the integral part in the CSCMR-WPT. Then, the optimal design parameters of the resonator loop as well as the source/load loop were derived and printed in the command window (MATLAB). The generated results were accurate well within the 5% error. Also, the capacitor-loaded and the self-resonant CSCMR-WPT models are discussed. It is shown clearly from the data provided that a self-resonant CSCMR-WPT performed better than the capacitor-loaded one, this is due to the self-resonant model having two layers which means the inductance of the loop becomes twice that of a single-layer. Furthermore, the inductance has a direct influence on mutual inductance which in turn affects the coupling coefficient. This means that the 2-layer resonator system has stronger coupling than a single-layer system, hence the higher transmission efficiency.

Chapter 4

Results and Discussions

From the previous chapter, two set of loops were derived. The resonator loop which in this case will be used as the transmitter (Tx) and the receiver (Rx) with the same dimensions were realised from the set of data provided in chapter 3 section 3.2. The source and the load loops with the same geometrical dimensions were also derived. In this section an optimal CSCMR-WPT system will be developed through systematic analysis. Section 4.1 presents the details for using co-simulation in an optimisation. Thereafter, specific data and the effects of using co-simulation compared to only using a full-wave electromagnetic simulations are discussed in section 4.2. The sensitivity analysis and optimisation are performed in section 4.3. Lastly, section 4.4 presents the effect of substrate on the transmission efficiency and the resonant frequency of a CSCMR-WPT system.

4.1 Optimal CSCMR-WPT System using Co-simulation

To design a practical yet optimal CSCMR-WPT system for small sensor devices (i.e., LPWAN devices), the physical dimensions of the WPT coils/loops need to be fairly miniature. The dimensions of this system can be scaled up or down as per requirement of a specific application. For consistency and based on existing low power sensor devices, the size of the proposed WPT system is kept at 100 mm. The CSCMR-WPT

system is realised in a way that the source/load loops sit concentrically within the transmitter/receiver resonators, this however poses a challenge when the loops are resized to achieve optimal performance, there is less room for the source and load loops. Therefore, to realise the highest practicable transmission efficiency, the critical parameters of the CSCMR-WPT system need to be optimised. For that to be achieved, the quality factor of the individual resonator, mutual coupling between resonators, frequency splitting phenomenon for the entire WPT system and input impedance of the system need to be critically studied and analysed with an accurate equivalent circuit model of the proposed CSCMR-WPT system.

With specified size constraints, critical design parameters such as the dimensions of the source/load loops, the dimensions of the Tx/Rx resonators which are dependent on but not limited to, the width (W), thickness (T), outermost diameter (d_{out}), are derived to yield optimal transmission efficiency of the CSCMR-WPT system with specified size constraints through systematic design process. The transmitter (Tx) and receiver (Rx) are designed to transmit maximum power transfer efficiency at a separation of 100 mm and based on the fact that the system is designed to provide efficient WPT for low power sensor devices with small footprint, the maximum dimensions for both the Tx and Rx of the system are constrained to 100 mm. The MATLAB derived model has identical resonators (Tx, Rx), as well as the source and load loops. This makes the analysis and assumptions less complex and also saves computational costs. Furthermore, to sustain a satisfactory quality factor of the source/load loop, [103] suggested that Q-source/load has to be greater than $1/Qresonator^{1/2}$; therefore, in order to leave adequate space for the source/load loop, the resonator's inner radius has to be limited.

Input impedance of the whole WPT system is another design factor that is of paramount importance, and it greatly depends on mutual coupling which in turn depends on the self-inductance and separation of the loops. The outermost diameter d_{out} has significant effect

on the frequency-splitting phenomenon, since an extremely large impedance angle and a relatively low amplitude will reduce efficiency [104]. As a result, for optimum performance, an optimal radius of the source/load loops must be defined for the proposed design. Figure 3.12 shows the methodical technique used in this work for the CSCMR-WPT system's analytical architecture.

In order to achieve a fully conformal system which has a small footprint, and which can easily be utilised for compact device applications, our proposed design uses conformal loops for both the source/load and resonators Tx/Rx. Also, the initial geometric parameters of the CSCMR loops are defined to be $d_{out} = 95.5mm$, $d_{outsource/load} = 59.7mm$, $W = 6mm$, $T = 0.03mm$. In order to have an efficient yet accurate simulation analysis and optimisation where less computational resources are used and at a shorter simulation time, some factors need to be taken into consideration.

4.2 Co-simulation

Simulations run using full-wave electromagnetic to determine the mutual coupling since other coupling parameters requires high computational costs. In this work, for the capacitor-loaded CSCMR, with the source/load loop with thickness of 0.035mm, width of 6mm and the outermost diameter of 87mm as depicted in Figure 3.4, using HFSS alone as the primary simulation software, the computational time required to run a full-wave simulation with reasonably fine-mesh is around 95 minutes with a custom build computer equipped with AMD Ryzen 5 1600 six-Core Processor with 3.20 GHz CPU and 16 GB RAM. This computational time becomes more than twice as long (220 minutes) when the model simulated is a 2-layer self-resonant CSCMR shown in Figure 3.10 with the same physical dimensions as the capacitor-loaded model. To optimise all important design parameters for both the capacitor-loaded and the 2-layer self-resonant CSCMR-WPT designs (e.g., the width of the loop, the dimension of the source and load loop, thickness

of the loop and the outermost diameter), the full-wave electromagnetic simulation would require high computational cost as well as simulation time.

To overcome this challenge, a co-simulation between HFSS and OptiSLang is used in this work. First, the influence of different physical parameters for the resonators and the source/load loops is studied using the derived formulae on MATLAB. Then, HFSS is used to determine the self-inductance (L) and the quality factor (Q) of the resonator loop. With the dimensional restrictions considered, a co-simulation between HFSS and OptiSLang is performed to determine the best fit values of the source/load loops (source and load loops are the same dimensions) for the highest achievable transmission efficiency analytically. The optimisation entails Sensitivity analysis which provides a clearer view on the selected parameters to be optimised for the MATLAB derived WPT (conventional) system. In this analysis, the effects as well as the percentage influence of each parameter with respect to given outputs/goals is observed. This assists in that it can be noticed if there are any tradeoffs that should be considered between the outputs/goals. In the sensitivity and optimisation analysis, a combination of the inner diameter and the outermost diameter of the loop is termed startHelix (SH) which is easily understood by the co-simulation. The loops are then fine-tuned in HFSS then the transmission efficiency is determined. Sensitivity analysis as well as the optimisation procedure are described next.

4.3 Sensitivity analysis and optimisation

This simulation can first be performed using ANSYS HFSS tool which is favourably suited to perform such simulations:

- For WPT simulations, HFSS has a frequency domain solver that has proven to be very efficient.
- optimum tradeoff between computational effort and physical and geometric accu-

racy is permissible by the finite element method which uses a conformal mesh.

- Its adaptive meshing reduces the impact of numerical errors on performance and guarantees numerical precision in parametric studies instinctively.

It is necessary to comprehend the dependencies of the quantities of interest on various parameters in order to optimise the design. Conversely, it becomes quite a complex task for this number of parameters to do by hand. In order to overcome this challenge, an optimisation tool like OptiSLang in co-simulation with HFSS can be utilised. OptiSLang, which employs Latin hypercube sampling, allows for a fully automated design of experiments with a fair number of samples, resulting in a very evenly distributed sampling of the design.

On the basis of these sampling links between geometric parameters and outcome quantities, a Meta Model of Optimal Prognosis (MOP) can be found (see Figure 4.1, Figure 4.2a and Figure 4.2b). The response surface for the result quantity under consideration is established by an MOP acquired by picking some 60% of the calculated design points. The Coefficient of Prognosis (CoP) is then determined through the remaining 40% of the calculated design points which are used to establish the quality of the response surface. OptiSLang divides the design points in a variety of ways, and the response surface with the best CoP is chosen as the MOP. The MOP can be used for optimisation if the prognosis quality is satisfactory, i.e., When carrying out the optimization, no new points must be determined using numerical simulation. The MOP is instead used to predict the results for the relevant design points. This technique makes OptiSLang very effective in that the optimisation run is quickened.

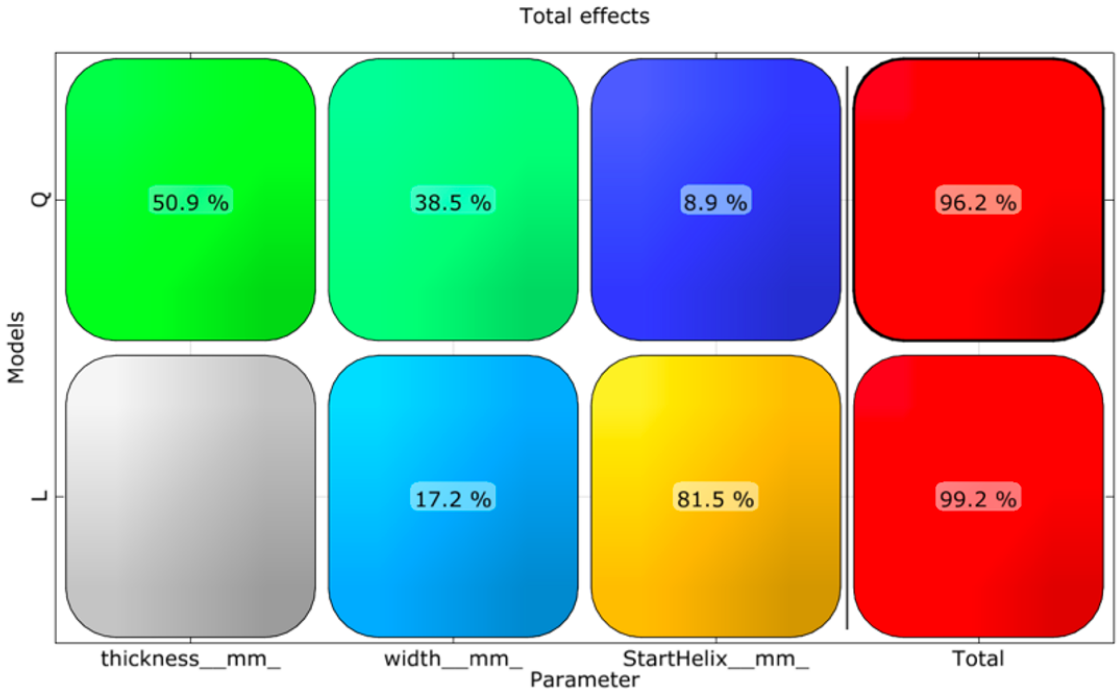

Figure 4.1: Meta Model of Optimal Prognosis, total parameter effect.

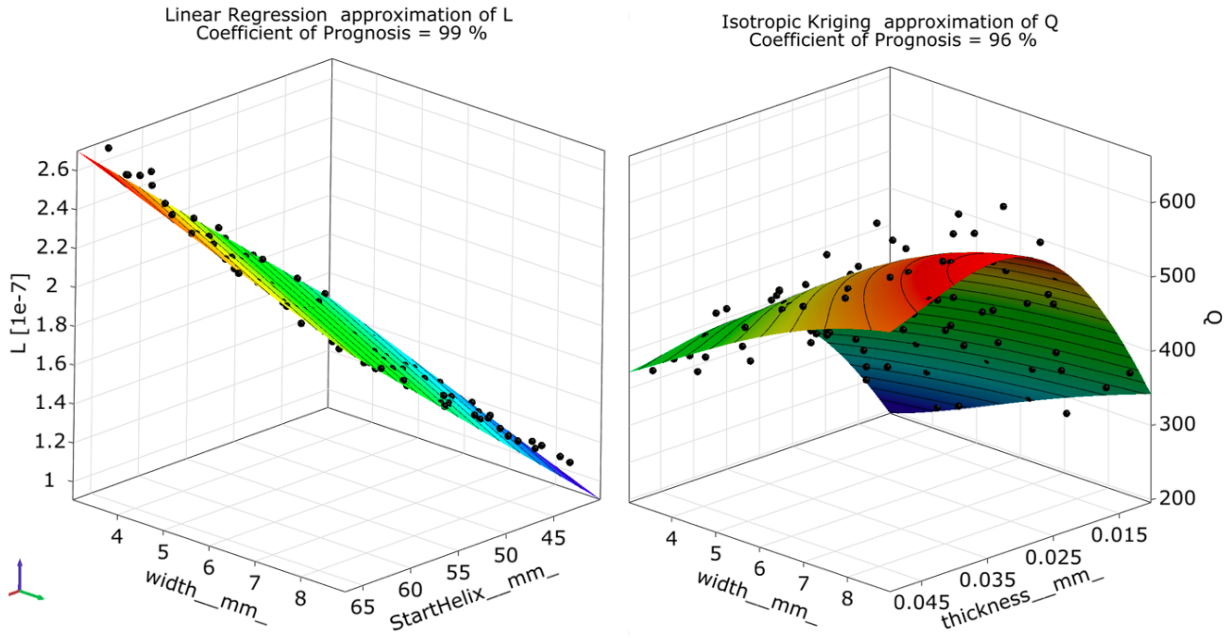

(a) (b)

Figure 4.2: Meta Model of Optimal Prognosis, (a). Coefficient of Prognosis (L), (b). Coefficient of Prognosis (Q).

Figure 4.2a depicts relationship between different input and output quantities. There

is for instance a rather strong, non-linear relationship between the startHelix (SH) and the self-inductance (L) of the loop, while the relationship between the quality factor (Q), SH and W also shows a non-linear relationship (Figure 4.1). Figure 4.2a and Figure 4.2b show the meta model of optimal prognosis for L and Q respectively, it depicts this linear and non-linear behaviour, and it has good and fair CoP of 99% (L) and 96% (Q). This shows that during the optimisation a tradeoff between Q and L can be considered. For this reason, considering the CoP, the MOP for this quantity is good enough to run an optimisation on. Therefore, a direct optimisation will not be run from our derived model as the MOP is strong enough to run the optimisation.

The optimisation goal for the model proposed in this work can be formulated using the quantities that are better behaved which directly depend on the physical dimensions of the model: the scattering parameters (S-param) of which Q plays a major role i.e., the positions of the maxima of the forward transmission coefficient (S21) usually behave in a much more predictable manner and the values of the S21 at the maxima also behave better. Once determined, S21 can be used to calculate the transmission efficiency of the WPT system. First, the optimisation is performed to enhance the derived MATLAB Tx/Rx resonators to attain a higher quality factor (Q), self-inductance is also taken into consideration as it plays a major role in mutual coupling. Then, the source/load loops are parametrically modified in HFSS with respect to the optimised Tx/Rx resonators to lessen the frequency-splitting phenomenon and improve the whole CSCMR system's transmission efficiency with the given constraints. Figure 4.3a and 4.3b show optimisation results of the best design attained from HFSS-OptiSLang co-simulation.

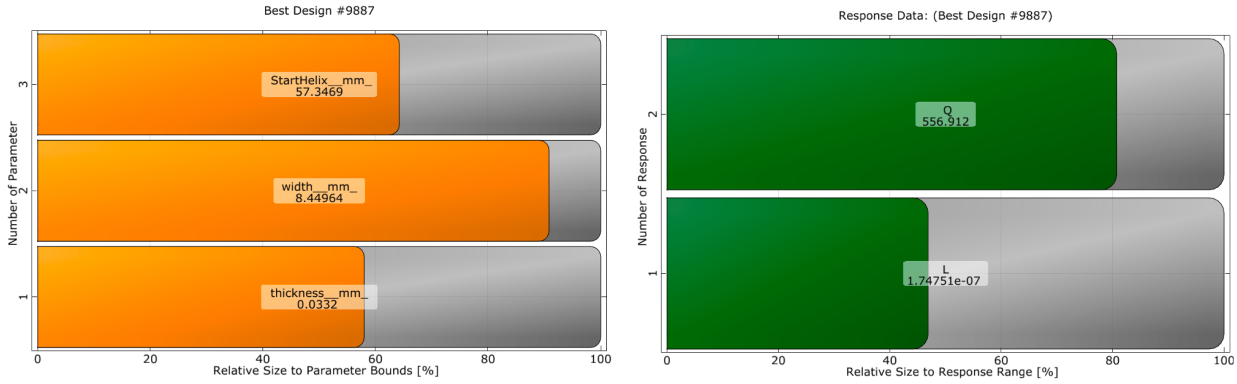

(a) (b)

Figure 4.3: Best design optimisation outputs. (a). optimised loop dimensions, (b). depicted tradeoff of L and improved Q.

By running the optimisation processes with CSCMR resonators of different geometrical parameters (d_{out}, W, T), we found that the increase in the outermost diameter and width of the loop yielded higher quality factor, which in turn gave the highest peak in transmission efficiency. While the increase in the outermost diameter and width of the loop improves the quality factor, an increase beyond certain limits, based on our design constraints, causes severe frequency-splitting which is contributed by impedance mismatch. The other carefully considered decision was having both L and Q as objective functions to be maximised, this was to have an automatic restriction on the loop to avoid the optimised resonator filling up the inner radius in a quest to find the highest Q. To be specific, from Figure 4.3a it is clearly depicted that the MATLAB derived CSCMR model has been enhanced, the overall footprint is reduced from 95.5 mm (d_{out}) to 88.7 mm, the width (W) has been increased by 10% while the thickness (T) has been slightly reduced by 5%. The resulting effects on the output variables sees the quality factor (Q) being increased by 30% from the initial value of 427, and self-inductance is reduced from 0.234 uF to 0.174 uF. The optimised parameters of the conformal strongly coupled magnetic resonance (CSCMR) WPT are then fine-tuned with HFSS to further improve the efficiency of the design, which then can be ready for fabrication if required. The finalised design parameters of the proposed CSCMR-WPT system are shown in Table 4.1.

Table 4.1: RLC values, design parameters.

Parameters	Tx/Rx Resonator Loop	Source/Load Loop
T (mm)	0.0332	0.0275
W (mm)	8.45	6
d_{out} (mm)	88.7	47.012
C_{Tx}, C_{Rx} (pF)	81	-
Q(unloaded) @40.68MHz	556	701
f_{max} (MHz)	40	89
L (uH)	0.175	0.113
R_S, R_L (ohm)	-	50

The optimised model derived from MATLAB was built in HFSS. The systems are run in the simulation that is real-like, the medium in which the loops are simulated is air. The optimised resonator coil was also used to develop an optimised 2-layer self-resonant CSCMR-WPT system as well. The self-resonant model performs well in environments where there are less resonating materials/devices and as mentioned before, there is no need to utilise capacitors so the system does not have capacitive losses. From Figure 4.4, the comparison of the MATLAB derived, 2-layer self-resonant developed from derived resonators and their optimised versions are presented. It is apparent from the results that the optimised MATLAB WPT performs far better than the originally derived one. This is due to the low Q-factor exhibited by the derived model and factors like the ratio of the Tx/Rx resonator loop to the source/load loop.

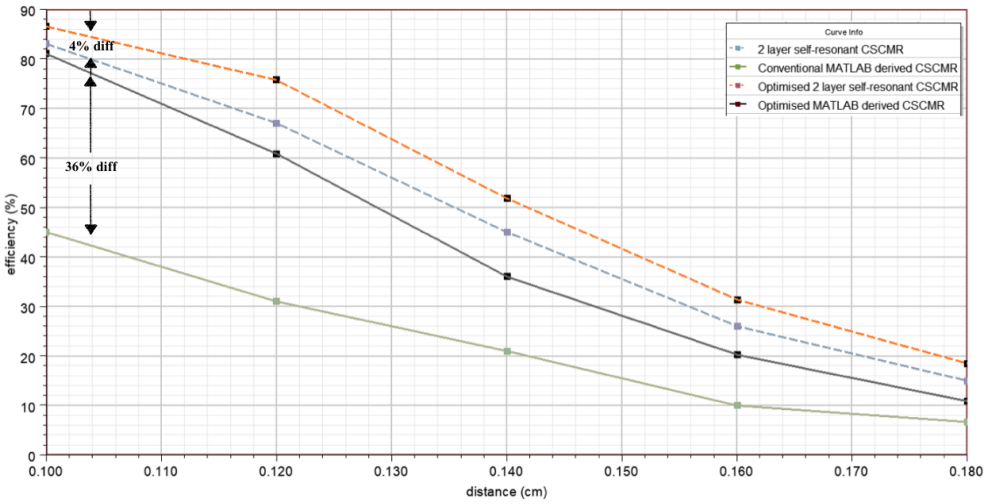

Figure 4.4: Comparison of the Matlab derived CSCMR-WPT system and its developed 2-layer self-resonant with their optimised versions.

The optimised derived model attains a transmission efficiency of 81% from 45% at 100 mm while its footprint is reduced from d_{out} 95.5 mm to 88.7 mm. With the optimised MATLAB derived model, the optimised 2-layer self-model was also realised and showed an improvement as well from its first model. Furthermore, the self-resonant model moved from 83% to 87% transmission efficiency also keeping a small footprint with the resonators' outermost diameter (d_{out}) of 88.7 mm with the height (h) of 0.55 mm between the two layers. Considering the co-simulation and the overall computational resources when compared to only running a full-wave electromagnetic simulation, it is clear that the co-simulation is more suitable. The total computational time for each simulation with a relatively fine-mesh is reduced to 15 minutes using the co-simulation. Compared to the initial time of 220 minutes this is an improvement of 93% simulation time needed for a full-wave simulation (refer to section 4.2).

4.4 Effects of Substrate

To have the CSCMR system closer to practical version, it is important to have the loops printed on a substrate. For the sake of consistency, the same models presented in Figure 3.2 and Figure 3.9 with the same dimensions are printed on an FR4 substrate with the

dimensions of 100mm x 100mm x 1.5mm (Figure 4.5).

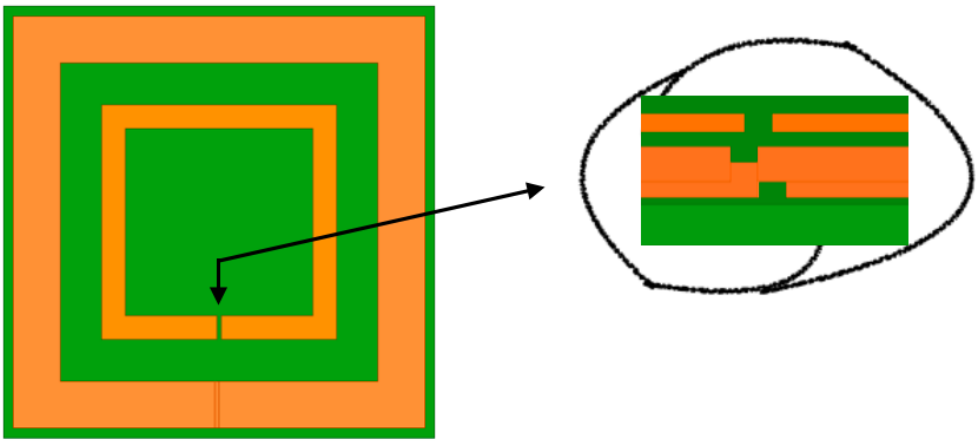

Figure 4.5: A substrate inclusion, 2-layer self-resonant CSCMR.

The scattering parameters (S_{21}) from which the efficiency can calculated as S_{21}^2, are shown in Figure 4.6 and Figure 4.7 for the CSCMR systems. In the presented results, it can be observed that the substrate has negligible effect on the transmission efficiency of both the capacitor-loaded and 2-layer self-resonant CSCMR designs. Conversely, the inclusion of the substrate with the specified dimensions moves the resonant frequency of the CSCMR systems to a lower frequency. To be exact, there is shift of 0.38 MHz from the set 40,68 MHz operating frequency for the capacitor-loaded design and a shift of 0.58 MHz for the 2-layer self-resonant CSCMR design. These observations are conclusive that the inclusion of the substrate (in this case an FR4) has a slight but notable effect on the resonant frequency of the CSCMR. These frequencies can be adjusted by fine tuning the resonator capacitors (for capacitor-loaded) and the height of the two layers (for 2-layer self-resonant) to get the required resonant frequency. Therefore, CSCMR can be printed on a substrate for fabrication without sacrificing the transmission efficiency of the system. The 3D view of the printed 2-layer self-resonant CSCMR system which has the same substrate as the capacitor-loaded system are shown in Figure 4.5 .

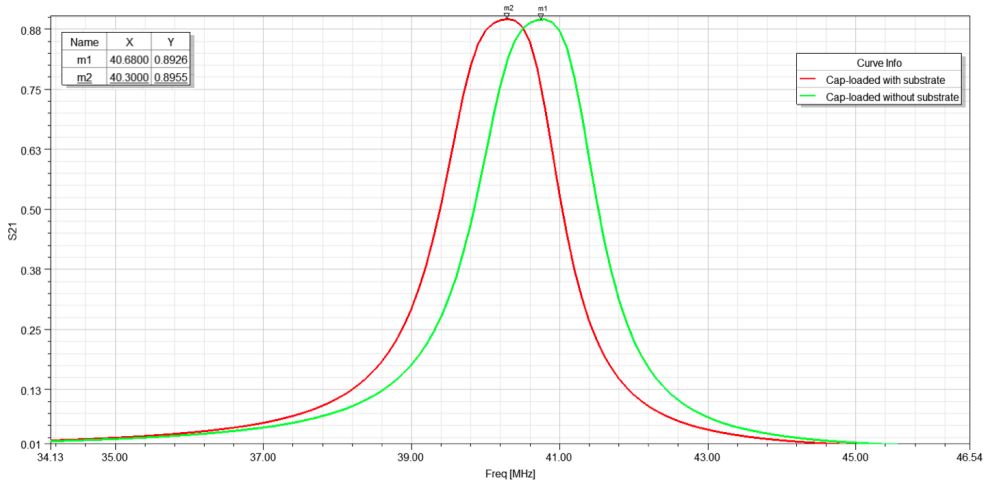

Figure 4.6: The effect of a substrate on a capacitor loaded model.

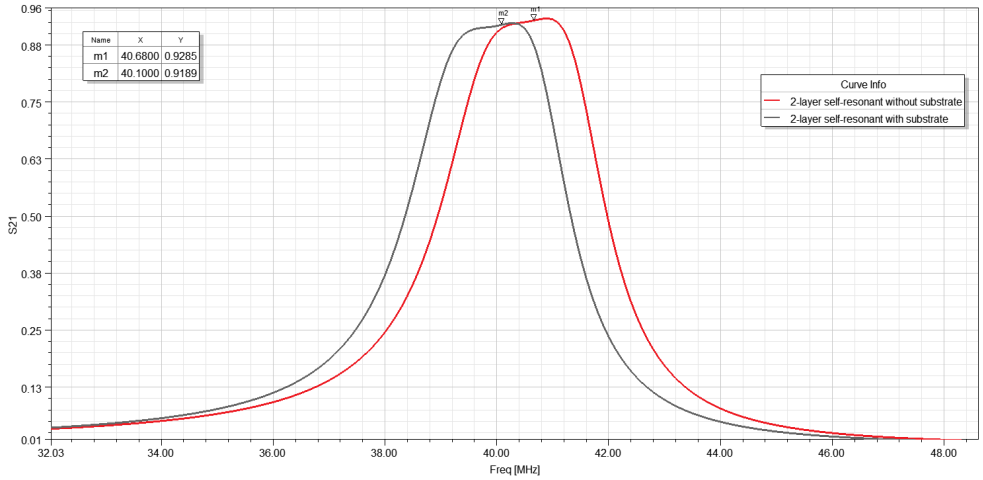

Figure 4.7: The effect of a substrate on a 2-layer self-resonant model.

4.5 Summary

In this chapter, a systematic method of optimisation was also elaborated together with the sensitivity and optimisation results. It was clearly shown that after a co-simulation of OptiSLang and HFSS, the overall dimensions of the resonators were reduced, which in turn reduced the entire CSCMR-WPT system footprint. This was done while the Q-factor was improved by 30% and the self-inductance of the resonator loop was reduced by 5%. The complete optimised WPT systems for a single and a 2-layer resonator were compared and the results showed high improvement in the conventional single-layer CSCMR, while

the 2-layer was also improved. The use of co-simulation proved to be an advantage in that the simulation time to run the optimisation was reduce to 7.32% compared to only using the full-wave electromagnetic simulation (HFSS). The effect of the substrate was also studied. It was found that the FR4 substrate slightly affects the resonant frequency, while the effect of its inclusion in the system has negligible effects on the transmission efficiency for both the capacitor-loaded and the 2-layer self-resonant CSCMR-WPT systems.

Chapter 5

Conclusions and Future Work

5.1 Conclusion

The objective of this dissertation was to develop WPT systems suitable for low power wide area network devices. The conformal strongly coupled magnetic resonance was the method chosen to achieve the goal because of its small footprint and suitability for low-power and compact-size applications with the ability to be operated in the Industrial, Scientific and Medical bands. Different WPT techniques were discussed in this dissertation. This was followed by a systematic view on their applications and the standards that regulates these WPT techniques. Two CSCMR-WPT systems were derived and analysed in this dissertation. These derived systems were proposed to take advantage of the previously proposed WPT systems and avoid some of their drawbacks. Equivalent circuit models were used for mathematical analysis. The mathematical analysis helped in evaluating different physical and electrical parameters of a WPT system and made it possible to see what influence one parameter had on the whole WPT system. These derived mathematical formulae were then applied in MATLAB with some functions in order to yield an optimal resonator loop which is the integral part in the CSCMR-WPT. Thereafter, the optimal design parameters of the resonator loop as well as the source/load loop were derived and printed in the command window (MATLAB). With the generated

results, 3D model with those specified dimensions was realised in HFSS. Thereafter, the capacitor-loaded and the self-resonant CSCMR-WPT models were evaluated. It was shown clearly from the data provided that a self-resonant CSCMR-WPT performed better than the capacitor-loaded one, this is due to the self-resonant model having two layers which means the self-inductance of the loop becomes twice that of a single-layer. Furthermore, the self-inductance has a direct influence on mutual inductance which in turn affects the coupling coefficient. This means that the 2-layer resonator system has stronger coupling than a single-layer system, hence the higher transmission efficiency. A systematic method of optimisation was also elaborated together with the sensitivity and optimisation results. It was clearly shown that after a co-simulation of OptiSLang and HFSS, the overall dimensions of the resonators were reduced, which in turn reduced the entire CSCMR-WPT system footprint. The derived single loop and 2-layer resonator CSCMR-WPT systems were able to achieve their optimal power transfer efficiency after sensitivity analysis and optimisation, at 100 mm with dimensions of 0.0332 mm, 8.45 mm, 88.7 mm for the resonator loops (Tx/Rx) and 0.0275 mm, 6 mm, 47.012 mm for the source/load loops. To be specific, the optimised derived model attained a transmission efficiency of 81% from 45% at 100 mm distance, while its footprint was reduced from d_{out} 95.5 mm to 88.7 mm, complying with the set restriction of 100mm. The optimised 2-layer self-model was also realised and showed an improvement of 4% compared to its initial model. Also, the self-resonant model moved from 83% to 87% transmission efficiency also keeping a small footprint with the resonators' outermost diameter (d_{out}) of 88.7 mm with the height (h) of 0.55 mm between the two layers. This was done while the Q-factor was improved by 30% and the self-inductance of the resonator loop reduced by 5%. The optimised WPT systems for a single layer (capacitor loaded) and a 2-layer resonator (self-resonant) were compared according to their transmission efficiency and the results showed high improvement for the conventional single-layer CSCMR, while the 2-layer was also improved. The use of co-simulation proved to be an advantage in that the simulation time to run the optimisation was reduced to 7.32% compared to only

using the HFSS. The effect of the substrate was also studied. It was found that the FR4 substrate slightly affects the resonant frequency, while the effect of its inclusion in the system has negligible effects on the transmission efficiency for both the capacitor-loaded and the 2-layer self-resonant CSCMR-WPT systems. To be exact, there was shift of 0.38 MHz from the set 40,68 MHz operating frequency for the capacitor-loaded design and a shift of 0.58 MHz for the 2-layer self-resonant CSCMR design.

In conclusion, the work done in this dissertation is (1) innovative in the structure design of the transmitter and receiver, (2) saves computational times and resources by using a code to realise WPT resonators and then using co-simulations to speed up optimisation processes and analysis. Overall, the proposed systems are suitable candidates for wireless charging of low power sensor devices.

5.2 Future Work

This research was centred on wireless power transfer optimisation for low power wide area networks applications by developing resonators with small footprint developed through less computational intense methods. However, future work is required in some areas.

The first part of this work focused on systematic optimisation of CSCMR physical dimensions and electrical parameters. Since the overall dimensions of our CSCMR-WPT system was limited to certain dimensions, more work can be done to further miniaturise the geometries for non-homogenous interface like medical implantable devices which are fairly small. This can be achieved with a combination of distinctive dielectrics and ferromagnetic materials whose permeability are very high, to attain an ideal small footprint embedded structures with noticeable system efficiency.

Additionally, the chunk of this research is to exploit ways of increasing the power

transmission efficiency to low power sensor devices and lessen the required battery charging times. The work can be stretched to the optimisation of these sensor devices so that they are completely passive and battery-less.

Finally, the derived and optimised models analysed in this work were not fabricated and physically tested. This research can be extended to analysis of the parameters using measuring tools like the vector network analyser. Also, the self-resonant CSCMR-WPT can be assessed on its performance when there are resonating materials and devices in its vicinity.

References

[1] A. Overmars and S. Venkatraman. "Towards a Secure and Scalable IoT Infrastructure: A Pilot Deployment for a Smart Water Monitoring System." *Technologies*, vol. 8. no. 4, pp. 50, **2020**.

[2] A. J. Ferguson, R. Woods, and D, Hester. "Towards Improved Sensor Systems for Bridge Structural Health Monitoring." *Civil Engineering Research in Ireland 2020*, pp. 21–26, **2020**.

[3] S. D. Glaser, M. Li, M. L. Wang, J. Ou, and J. Lynch. "Sen-sor technology innovation for the advancement of structural health monitoring: A strategic program of US-China research for the next decade." *Smart Structures and Systems*, vol, 3, no. 2, pp. 221–244, **2007**.

[4] L. La Blunda, L. Guti´errez-Madron˜al, M. F. Wagner, and I. Medina-Bulo. "A Wearable Fall Detection System Based on Body Area Networks." *IEEE Access*, vol. 8, no. 3, pp. 193060–193074, **2020**.

[5] T. J. Bernhard, K. Hietpas, E. George, D. Kuchma, and H. Reis. An Interdisciplinary effort to develop a wireless embedded sensor system to monitor and assess corrosion in the tendons of prestressed concrete girders. *2003 IEEE Topical Conference on Wireless Communication Technology*, pp 241–243, **2003**.

[6] M. Bhagat, and S. Nalbalwar. Wireless Transfer of Solar Power for Charging Mobile Devices in a Vehicle. *In International Conference on Communication and Signal Processing 2016 (ICCASP 2016)*, vol. 137, pp 673-677, **2017**.

[7] M. Rozman. *Inductive Wireless Power Transmission for Automotive Applications*. PhD thesis, Manchester Metropolitan University, **2019**.

[8] J. C. Maxwell. *A treatise on electricity and magnetism*. Oxford: Clarendon Press, **1873**.

[9] F. Marra, L. Zhang, and J. G. Lyng. "Radio frequency treatment of foods: Review of recent advances." *Journal of Food Engineering*, vol. 91, no. 4, pp. 497-508, **2009**.

[10] A. S. Marincic. "Nikola tesla and the wireless transmission of energy." *IEEE Transactions on Power Apparatus and Systems*, no. 10, 4064 - 4068, **1982**.

[11] C. K. Lee, and W. X. Zhong. Recent Progress in Mid-Range Wireless Power Transfer. *In 2012 IEEE Energy Conversion Congress and Exposition (ECCE)*, pp. 3819-3824. IEEE, **2012**.

[12] S. C. Nambiar and M. Manteghi . A simple wireless power transfer scheme for implanted devices. *In: 2014 United States National Committee of URSI Nat. Radio Science Meeting (USNC-URSI NRSM)*, pp. 1-1, **2014**.

[13] E.C. Okress, W.C. Brown, T. Moreno, G. Goubau, N.I. Heenan, and R.H. George. Microwave power engineering. *In: IEEE Spectrum* 1.10 (1964), pp. 76-76, **1964**.

[14] B. Strassner, and K. Chang. Microwave power transmission: Historical mile- stones and system components. *Proceedings of the IEEE 101*, vol. 101, no. 6, pp. 1379-1396, **2013**.

[15] J. O. McSpadden, and J.C. Mankins. "Space solar power programs and microwave wireless power transmission technology." *IEEE Microwave Magazine*, vol. 3, no. 4, pp. 46-57, **2002**.

[16] A.K. RamRakhyani, S. Mirabbasi, and M. Chiao. "Design and optimization of resonance-based efficient wireless power delivery systems for biomedical implants." *IEEE Transactions on Biomedical Circuits and Systems*, vol. 5, no. 1, pp. 48-63, **2011**.

[17] X. Lu, P. Wang, D. Niyato, D.I. Kim, and Z. Han. "Wireless Charging Technologies: Fundamentals, Standards, and Network Applications." *IEEE Communications Surveys and Tutorials*, vol. 18, no. 2. pp. 1413–1452, **2016**.

[18] F. Wen, X. Chu, Q. Li, R. Li, L. Liu, and F. Jing. "Optimization on Three-Coil Long-Range and Dimension-Asymmetric Wire- less Power Transfer System." *IEEE Transactions on Electromagnetic Compatibility*, vol. 62, no. 5, pp. 1859-1868, **2020**.

[19] G. Kiruthiga, M.Y. Jayant, and A. Sharmila. "Wireless charging for low power applications using Qi standard." *In 2016 International Conference on Communication and Signal Processing (ICCSP)*, pp. 1180–1184, **2016**.

[20] Y.J. Park, B. Jang, S.M. Park, H.C. Ryu, S.J. Oh, S.Y. Kim, Y. Pu, S.S. Yoo, K.C. Hwang, Y. Yang, and M. Lee. "A triple-mode wireless power-receiving unit with 85.5% system efficiency for A4WP, WPC, and PMA applications." *IEEE Transactions on Power Electronics*, vol. 33, no. 4, pp. 3141–3156, **2018**.

[21] T. Yilmaz, N. Hasan, R. Zane, and Z. Pantic. "Multi-Objective Optimization of Circular Magnetic Couplers for Wireless Power Transfer Applications." *IEEE Transactions on Magnetics*, vol. 53, no. 8, pp. 1-12, **2017**.

[22] C.R. Dietlein, A.S. Hedden, and D.A. Wikner. "Digital reflectarray considerations for terrestrial millimeter-wave imaging." *IEEE Antennas and Wireless Propagation Letters*, vol. 11, pp.272-275, **2012**.

[23] W. Huang, B. Zhang, X. Chen, K. Huang, and C. Liu. Study on an S-band rectenna array for wireless microwave power transmission. *Progress in Electromagnetics Research*, vol. 135, no. December 2012, pp. 747-758, **2013**.

[24] A. Ahmad, M.S. Alam, and R. Chabaan. "A comprehensive review of wireless charging technologies for electric vehicles." *IEEE Transactions on Transportation Electrification*, vol. 4, no. 1, pp. 38-63, **2018**.

[25] A. S. Hassan, R. T. Hussein, and I. K. "Abboud. Design and Implementation of a Wireless Power Transfer Network." *IOP Conference Series: Materials Science and Engineering*, vol, 870, no. 1, pp. 012131, **2020**.

[26] M. M. Zhao, Q. Shi, and M. J Zhao. "Efficiency Maximization for UAV-Enabled Mobile Relaying Systems with Laser Charging." *IEEE Transactions on Wireless Communications*, vol. 19. no. 5, pp. 3257-3272, **2020**.

[27] S. M. Kim, and H. Park. "Optimization of optical wireless power transfer using near-infrared laser diodes." *Chinese Optics Letters*, vol. 18, no. 4, pp. 042603, **2020**.

[28] V. B. Keerthi, V. Swetha, and E. Annadevi. "Wireless Power Transmission." *IOP Conference Series: Materials Science and Engineering*, vol. 590, no. 1, pp. 444-449, **2019**.

[29] Q. Zhang, W. Fang, Q. Liu, J. Wu, P. Xia, and L. Yang. Distributed Laser Charging: A Wireless Power Transfer Approach.*IEEE Internet of Things Journal*, vol, 5, no. 5, pp. 3853-3864, **2018**.

[30] J. Cheng, J. Wang, E. Peng, H. Yang, H. Chen, M. Chen, and J. Tan. Combined modulation of incident laser light by multiple surface scratches and their effects on the laser damage properties of KH 2 PO 4 crystal. *Optics Express*, vol, 28, no. 6, pp. 8764, **2020**.

[31] A. Le, L. Truong, T. Quyen, C. Nguyen, and M. Nguyen. "Wireless Power Transfer Near-field Technologies for Unmanned Aerial Vehicles (UAVs): A Review." *EAI Endorsed Transactions on Industrial Networks and Intelligent Systems*, vol. 7, no. 22, pp. 162831,**2020**.

[32] Z. Pantic, and S.M. Lukic. "Framework and topology for active tuning of parallel compensated receivers in power transfer systems." *IEEE Transactions on Power Electronics*, vol. 27, no. 11, pp. 4503-4513, **2012**.

[33] D. Ustun, S. Balci, and K. Sabanci. "A parametric simulation of the wireless power transfer with inductive coupling for electric vehicles, and modelling with artificial bee colony algorithm." *Measurement: Journal of the International Measurement Confederation*, vol. 150, pp. 107082, **2020**.

[34] T. Hiramatsu, X. Huang, M. Kato, T. Imura, and Y. Hori. Wireless charging power control for HESS through receiver side voltage control. *Conference Proceedings - IEEE Applied Power Electronics Conference and Exposition - APEC, 2015 - (May)*, pp 1614-1619, **2015**.

[35] F. Musavi, M. Edington, and W. Eberle. "Wireless power transfer: A survey of EV battery charging technologies." *2012 IEEE Energy Conversion Congress and Exposition (ECCE)*, pp. 1804-1810, **2012**.

[36] S. Wang, J. Liang, H. Wang, and M. Fu. An Induced Voltage Source Model for Capacitive Power Transfer. *Conference Proceedings - IEEE Applied Power Electronics Conference and Exposition - APEC, 2020-March*, pp. 846-851, **2020**.

[37] J. Dai, and D.C. Ludois. A survey of wireless power transfer and a critical comparison of inductive and capacitive coupling for small gap applications. *In: IEEE Trans. Power Electron*, 30(11): pp. 6017-6029., **2015**.

[38] F. Lu, H. Zhang, and C. Mi. "A review on the recent development of capacitive wireless power transfer technology." *Energies*, vol. 10, no. 11, **2017**.

[39] S. R. Khan, S. K. Pavuluri, G. Cummins, and M.P. Desmulliez. "Wireless power transfer techniques for implantable medical devices: A review." *Sensors (Switzerland)*, vol. 20, no. 12, pp. 1-58, **2020**.

[40] F. Lu, H. Zhang, H. Hofmann, and C.C. Mi. "A Double-Sided LCLC - Compensated Capacitive Power Transfer System for Electric Vehicle Charging." *IEEE Transactions on Power Electronics*, vol. 30, no. 11, pp. 6011-6014, **2015**.

[41] F. Lu, H. Zhang, H. Hofmann, and C.C. M. "An inductive and capacitive combined wireless power transfer system with LC-compensated topology." *IEEE Transactions on Power Electronics*, vol. 31, no. 12, pp. 8471-8482, **2016**.

[42] A. Costanzo, M. Dionigi, F. Mastri, M. Mongiardo, G. Monti, J.A. Russer, P. Russer, L. Tarricone. Conditions for a load-independent operating regime in resonant inductive WPT. *IEEE Transactions on Microwave Theory and Techniques*, vol. 65, no. 4, pp. 1066-1076, **2017**.

[43] M. Rozman, M. Fernando, B. Adebisi, K. M. Rabie, R. Kharel, A Ikpehai, and H. Gacanin. "Combined conformal strongly- coupled magnetic resonance for efficient wireless power transfer." *Energies*, vol. 10, no. 4, pp. 1-18, **2017**.

[44] K. Hassan, S. Pan, and P. Jain. "Multiple receiver wire-less power charger for mobile electronic devices in near field." *In 018 IEEE International Conference on Industrial Electronics for Sustainable Energy Systems (IESES)*, pp. 426-433. IEEE, **2018**.

[45] J. Wang, C. Shen, P. Zhao, S. Ou, Z. Xu, R. Zhang, and Z. Song. "A Design Method for Magnetically Coupled Resonant Coils Considering Transmission Objectives and Dimension Constraints." *Energies*, vol. 13, no. 16, pp. 4144, **2020**.

[46] S.M. Kim, I.K. Cho, J.I. Moon, S.I. Jeon, and J.I. Choi. 5W wireless power transmission system with coupled magnetic resonance. *In 2013 5th IEEE International Symposium on Microwave, Antenna, Propagation and EMC Tech- nologies for Wireless Communication*, pp. 255-258, **2013**.

[47] M. Rozman, K. M. Rabie, and B. Adebisi. "Wireless Power and Communication Transmission for Industrial Robots." *In 2018 11th International Symposium on*

Communication Systems, Networks and Digital Signal Processing, CSNDSP 2018, pp 1-5, **2018**.

[48] S. Prengel, M. Helwig, and N. Modler. "Lightweight coil for efficient wireless power transfer: Optimization of weight and efficiency for WPT coils." *In 2014 IEEE Wireless Power Transfer Conference*, pp. 96-99, **2014**.

[49] B. Li, Y. Geng, F. Lin, Z. Yang, and S. Igarashi. "Design of constant voltage compensation topology applied to wpt system for electrical vehicles." *2016 IEEE Vehicle Power and Propulsion Conference (VPPC)*,!EEE: pp. 1-6, **2016**.

[50] Q. Gu, G. Wang, R. Fan, F. Li, H. Jiang, and Z. Zhong. "Optimal Resource Allocation for Wireless Powered Sensors: A Perspective from Age of Information." *IEEE Communications Letters*, pp 1-1, **2020**.

[51] N. Mohamed, F. Aymen, M. B. Hamed, and S. Lassaad. "Analysis of battery-EV state of charge for a dynamic wireless charging system." *Energy Storage*, vol. 2, no. 2, pp. 1-10, **2020**.

[52] M. Bertoluzzo, M. Di Monaco, G. Buja, G. Tomasso, and A. Genovese. "Comprehensive development of dynamic wireless power trans- fer system for electric vehicle." *Electronics (Switzerland)*, vol. 9, no. 6, pp. 1-20, **2020**.

[53] N. Shinohara. "Wireless power transmission progress for electric vehicle in Japan.' *In 2013 IEEE Radio and Wireless Symposium*, pp. 109-111,**2013**.

[54] H. Matsumoto. "Research on solar power satellites and microwave power transmission in Japan." *IEEE Microwave Magazine*, vol. 3, no. 4, pp. 36-45,**2002**.

[55] J. Chen, C. W. Yu, and W. Ouyang. "Efficient Wireless Charging Pad Deployment in Wireless Rechargeable Sensor Networks." *IEEE Access*, vol. 8, no. 2, pp. 39056–39077,**2020**.

[56] R. La Rosa, C. Dehollain, and P. Livreri. "Advanced monitoring systems based on battery-less asset tracking modules energized through rf wireless power transfer." *Sensors (Switzerland)*, vol,. 20. no. 11, pp. 3020, **2020**.

[57] T. V. Muni, A. S. Pranav, and A. A. Srinivas. "IoT based smart battery station using wireless power transfer technology." *International Journal of Scientific and Technology Research*, vol. 9, no. 1, pp. 2876-2881, **2020**.

[58] Z. Zhang, C. Chen, T. Fei, H. Xiao, G. Xie, and X. Cheng. "Wireless communication and wireless power transfer system for implantable medical device." *Journal of Semiconductors*, vol. 41, no. 10, pp. 0-7, **2020**.

[59] Y. Zhou, C, Liu, and Y, Huang. "Wireless power transfer for implanted medical application: A review." *Energies*, vol. 13, no. 11, pp. 2837, **2020**.

[60] K. A. Townsend, J. W. Haslett, T. K. K. Tsang, M. N. El-Gamal, and K. Iniewski. "Recent advances and future trends in low power wireless systems for medical applications." *Proceedings - Fifth International Work- shop on System-on-Chip for Real-Time Applications, IWSOC 2005*, 2005, pp. 476-481,**2005**.

[61] A. Lymberis. "Smart wearable systems for personalised health management: Current R&D and future challenges." *Annual International Conference of the IEEE Engineering in Medicine and Biology - Proceedings*, vol. 4, pp. 3716-3719, **2003**.

[62] P. Meshram, A Mishra, and R, Sahu. "Environmental impact of spent lithiumion batteries and green recycling perspectives by organic acids – A review." *Chemosphere*, vol. 242, pp. 125291, **2020**.

[63] C. Liu, A.P. Hu, and X. Dai. "A contactless power transfer system with capacitively coupled matrix pad." *In 2011 IEEE Energy Conversion Congress and Exposition*, pp. 3488-3494, **2011**.

[64] M. Kline, I. Izyumin, B. Boser, and S. Sanders. "Capacitive power transfer for contactless charging." *In 011 Twenty-Sixth Annual IEEE Applied Power Electronics Conference and Exposition (APEC)*, pp. 1398-1404. IEEE, **2011**.

[65] H. Ying, A. T. L. Lee, S. C. Tan, and S. Y. Hui. "Highly- Efficient Wireless Power Transfer System with Single-Switch Step-Up Resonant Inverter." *IEEE Journal of Emerging and Selected Topics in Power Electronics*, vol. 6777(c), pp. 1-1, **2020**.

[66] P. Ramezani and A. Jamalipour. "Throughput Maximization in Dual-Hop Wireless Powered Communication Networks." *IEEE Transactions on Vehicular Technology*, vol. 66, no. 10, pp. 9304-9312, **2017**.

[67] J. Choi, Y.H. Ryu, D. Kim, N.Y. Kim, C. Yoon and Yoon, Y.K. Park, S. Kwon, and Y. Yang. Design of high efficiency wireless charging pad based on magnetic resonance coupling. *In 2012 9th European Radar Conference*, pp. 590-593, **2012**.

[68] A.J. Onumanyi, A.M. Abu-Mahfouz, and G.P. Hancke. "Low Power Wide Area Network, Cognitive Radio and the Internet of Things: Potentials for Integration." *Sensors*, vol. 20, no. 23, pp. 6837, **2020**.

[69] N. Neo, E. D. Markus, M. Masinde, and A. M. Abu-Mahfouz. "Potable Water Quality Monitoring: A Survey of Intelligent Techniques." *In 2019 International Multidisciplinary Information Technology and Engineering Conference (IMITEC)*, pp. 1-6, **2019**.

[70] N. Koyana, E. D Markus, and A. M. Abu-Mahfouz. "A Survey of Network and Intelligent air pollution monitoring in South Africa." *Proceedings - 2019 International Multidisciplinary Information Technology and Engineering Conference, IMITEC 2019*, **2019**.

[71] J Jin, X. Wu, and Z. Li. "Ultra-low power mixer with out-of-band RF energy harvesting for wireless sensor networks applications." *Engineering Review*, vol. 40, no. 1, pp. 1-6, **2020**.

[72] F. Akhtar and M. H. Rehmani. "Energy replenishment using renewable and traditional energy resources for sustainable wireless sensor networks: A review." *Renewable and Sustainable Energy Reviews*, vol. 45, pp. 769-784, **2015**.

[73] N. Liu and B. Wang. "An LLC-based planar wireless power transfer system for multiple devices." *Conference Proceedings - IEEE Applied Power Electronics Conference and Exposition - APEC*, pp. 3411-3417, **2014**.

[74] S. Hached, A.Trigui, I. El Khalloufi, M. Sawan, O. Loutochin, and J. Corcos. "A bluetooth-based low-energy qi-compliant battery charger for implantable medical devices." *In 2014 IEEE International Symposium on Bioelectronics and Bioinformatics (IEEE ISBB 2014)*, pp. 1-4, **2014**.

[75] R. Tseng, B. Von Novak, S. Shevde, and K. A. Grajski. "Introduction to the alliance for wireless power loosely-coupled wireless power transfer system specification version 1.0." *2013 IEEE Wireless Power Transfer, WPT 2013*, pp. 79-83, **2013**.

[76] W. Li, P. Wang, C. Yao, Y. Zhang, and H. Tang. "Experimental investigation of 1D, 2D, and 3D metamaterials for efficiency enhancement in a 6.78 MHz wireless power transfer system." *In 2016 IEEE Wireless Power Transfer Conference (WPTC)*, pp. 1-4, **2016**.

[77] D. Bol, G. de Streel, and D. Flandre. :Can we connect trillions of IoT sensors in a sustainable way? A technology/circuit perspective." *In 2015 IEEE SOI-3D-Subthreshold Microelectronics Technology Unified Conference (S3S)*, pp. 1-3, **2015**.

[78] C.O. Mathu´na, T. O'Donnell, R. V. Martinez-Catala, J. Rohan, and B O'Flynn. "Energy scavenging for long-term deployable wireless sensor networks." *Talanta*, vol. 75, no. 3, pp. 613-623,**2008**.

[79] R. Dekimpe, P. Xu, M. Schramme, P. G´erard, D. Flandre, and D. Bol. "A battery-less BLE smart sensor for room occupancy tracking supplied by 2.45-GHz wireless power transfer." *Integration*, vol. 67, no. (February), pp. 8-18, **2019**.

[80] N.B. Carvalho, A. Georgiadis, A. Costanzo, H. Rogier, A. Collado, J. A. Garcia, S. Lucyszyn, P. Mezzanotte, J. Kracek, D. Masotti, A. J. S. Boaventura. "Wireless power transmission: R&D activities within Europe. *IEEE Transactions on Microwave Theory and Techniques*, vol. 62, no. 4, pp. 1031-1045, **2014**.

[81] F. Kilic, S. Sezen, and S. A Sis. "A misalignment-adaptive wireless power transfer system using PSO-based frequency tracking." *An International Journal of Optimization and Control: Theories & Applications (IJOCTA)*, vol. 10, no. 2, pp. 206, **2020**.

[82] A. Fereshtian and J. Ghalibafan. "Impedance matching and efficiency improvement of a dual-band wireless power transfer system using variable inductance and coupling method." *AEU - International Journal of Electronics and Communications*, vol, 116, pp. 153085, **2020**.

[83] Y. Zhaksylyk, U. Hanke, and M. Azadmehr. "Design of a switchable driving coil for Magnetic Resonance Wireless Power Transfer." *2019 IEEE PELS Workshop on Emerging Technologies: Wireless Power Transfer, WoW 2019*, pp. 249-252, **2019**.

[84] X. Wei, Z. Wang, and H. Dai. "A critical review of wireless power transfer via strongly coupled magnetic resonances." *Energies,* vol. 7, no. 7, pp. 4316-4341, **2014**.

[85] A. Kurs, A. Karalis, R. Moffatt, J. D. Joannopoulos, P. Fisher, and M. Solja˘ci´c. "Wireless power transfer via strongly coupled magnetic resonances." *Science*, vol, 317, no. 5834, pp. 83-86, **2007**.

[86] A. Karalis, J. D. Joannopoulos, and M. Solja˘ci´c. "Efficient wireless non-radiative mid-range energy transfer." *Annals of Physics*, vol. 323, no. 1, pp. 34-48, **2008**.

[87] M. Kiani and M, Ghovanloo. "The circuit theory behind coupled-mode magnetic resonance-based wireless power transmission." *IEEE Transactions on Circuits and Systems I: Regular Papers*, vol. 59, no. 9, pp. 2065-2074, **2012**.

[88] O. Jonah. *Optimization of Wireless Power Transfer via Magnetic Resonance in Different Media*. PhD thesis, Florida International University, University Park, Florida, United States, **2013**.

[89] F. Jolani, Y. Yu, and Z. Chen. "A planar magnetically coupled resonant wireless power transfer system using printed spiral coils." *IEEE Antennas and Wireless Propagation Letters*, vol. 13, pp. 1648-1651, **2014**.

[90] V. Nagoorkar. *Midrange Magnetically-Coupled Resonant Circuit Wireless Power Transfer*. PhD thesis, MS, The University of Texas, Tyler, United States, **2014**.

[91] S.S. Mohan, M. del Mar Hershenson, S.P. Boyd, and T.H. Lee. "Simple Accurate Expressions for Planar Spiral Inductances." *IEEE Journal of solid-state circuits*, vol. 34, no. 10, pp. 1419-1424, **1999**.

[92] C. A. Balanis. *Antenna Theory: Analysis and Design*. Canada, 4th ed. North America: John Wiley & Sons, **2016**.

[93] W. B. Kuhn and N. M. Ibrahim. "Analysis of current crowding effects in multiturn spiral inductors." *IEEE Transactions on Microwave Theory and Techniques*, vol. 49, no. 1, pp. 31-38, **2001**.

[94] G. K. Felic, D. Ng, and E. Skafidas. "Investigation of frequency- dependent effects in inductive coils for implantable electronics." *IEEE Transactions on Magnetics*, vol. 49, no. 4, pp. 1353-1360, **2013**.

[95] S. Raju, R. Wu, M. Chan, and C. P. Yue. "Modeling of mutual coupling between planar inductors in wireless power applications." *IEEE Transactions on Power Electronics*, vol. 29, no. 1, pp. 481-490, **2014**.

[96] H. Hoang and F, Bie. "Maximizing Efficiency of Electromagnetic Resonance Wireless Power Transmission Systems with Adaptive Circuits." *Wireless Power Transfer - Principles and Engineering Explorations*, **2012**.

[97] F, Jolani, Y. O Yu, and Z. D. Chen. "Electromagnetic modeling and optimization of magnetic resonant coupling wireless power transfer using coil array." *Proceedings of 2015 IEEE MTT-S International Conference on Numerical Electromagnetic and Multiphysics Modeling and Optimization, NEMO 2015*, vol, 1, pp. 1-3, **2016**.

[98] T. P. Truong, D. A. Duong, T. H. D. Nguyen, and L. V. Q. Danh. "Design and deployment of a LoRa-based wireless sensor network for structural health monitoring system." *International Journal of Smart Grid and Clean Energy*, pp. 83-91, **2020**.

[99] M. Abdulkarem, K. Samsudin, F. Z. Rokhani, and M. F. A. Rasid. "Wireless sensor network for structural health monitoring: A contemporary review of technologies, challenges, and future direction." *Structural Health Monitoring*, vol. 19, no. 3, pp. 693-735, **2020**.

[100] G. Wang and J. Sun. "Improved Magnetic Coupling Resonance Wireless Power Transfer System." *Chinese Control Conference, CCC*, 2020-July, pp. 5317-5321, **2020**.

[101] M.M.A. El Negm, H. A. Atallah, A. Allam, and A.B. Abd El Rahman. Sign of Compact Coupled Resonators for Triple Band Wireless Power Transfer (TB-WPT). *In IEEE Microwave and Wireless Components Letters*, pp. 1-1, **2021**.

[102] S. Zhang, W. Zhong, and D. Xu. "A Reconfigurable Resonant Topology of Wireless Power Transfer Systems with Large Coupling Ranges." *2020 IEEE 9th International Power Electronics and Motion Control Conference (IPEMC2020-ECCE Asia), Nanjing, China, 2020*, pp. 3281-3287, **2020**.

[103] A. P. Sample, D. A. Meyer, and J. R. Smith. "Analysis, experimental results, and range adaptation of magnetically coupled resonators for wireless power transfer." *IEEE Transactions on Industrial Electronics*, vol. 58, no. 2, pp. 544-554, **2011**.

[104] Y. Zhang, Z. Zhao, and K. Chen. "Frequency splitting analysis of magnetically-coupled resonant wireless power transfer." *2013 IEEE Energy Conversion Congress and Exposition, ECCE 2013*, pp. 2227-2232, **2013**.